



**João Filipe Pereira Domingues Alho**

Licenciado em Ciências da Engenharia Física

**Development of didactic physics experiments  
using a miniaturized wireless acquisition board**

Dissertação para obtenção do Grau de Mestre em  
**Engenharia Física**

Orientador: Grégoire Bonfait,  
Professor Associado com Agregação,  
Universidade Nova de Lisboa

Co-orientador: Hugo Silva,  
Chief Innovation Officer, PLUX - Wireless Biosignals,  
S.A.,  
Investigador, IT - Instituto de Telecomunicações

Júri

Presidente: Prof. Dr. Yuri Nunes  
Arguente: Prof. Dr. André Wemans  
Vogal: Prof. Dr. Hugo Silva



FACULDADE DE  
CIÊNCIAS E TECNOLOGIA  
UNIVERSIDADE NOVA DE LISBOA

September, 2017



## **Development of didactic physics experiments using a miniaturized wireless acquisition board**

Copyright © João Filipe Pereira Domingues Alho, Faculdade de Ciências e Tecnologia, Universidade NOVA de Lisboa.

A Faculdade de Ciências e Tecnologia e a Universidade NOVA de Lisboa têm o direito, perpétuo e sem limites geográficos, de arquivar e publicar esta dissertação através de exemplares impressos reproduzidos em papel ou de forma digital, ou por qualquer outro meio conhecido ou que venha a ser inventado, e de a divulgar através de repositórios científicos e de admitir a sua cópia e distribuição com objetivos educacionais ou de investigação, não comerciais, desde que seja dado crédito ao autor e editor.





*You did to life my noble impulse warm,  
Deep in the spirit of the world to look,  
And with your hand a trusting faith I took,  
Securely bearing me through every storm.*

*-Novalis*



## ACKNOWLEDGEMENTS

First and foremost, I would like to thank my adviser, Prof. Grégoire Bonfait, not only for his guidance, patience and commitment, but also for the opportunity to work with him. I must also extend these thanks to Prof. Hugo Silva, my co-adviser, who was always eager to help me in any way he could. The opportunity to work with so many different tools was absolutely enriching. It was a challenge that I can only be happy to have overcome with the help of my advisers.

Essential to this work was the help and equipment provided by PLUX. Without their commitment to this project this work would have simply not been possible. For this reason, I extend my thanks to them.

To my colleagues Diogo Silva, Jorge Barreto and Sofia Alves, who showed their unquestionable support and friendship, I wish to express my deepest gratitude. It is fair to say that without them this would have been a far more difficult challenge.

To my friends of long years, André Serrano, Diogo Maximino, Inês Salgado and João Brejo, I say thank you for many years of friendship and companionship. I am truly grateful to have such awe inspiring friends.

At last I thank my family. To my grandfather for setting this example of a caring, stout, hard-working man that I can only hope to one day match. To my grandmother for her unconditional love for her family, and many laughs and amazing meals. To my father for the reassurance and support. For instilling in me a calm and positive look on life. To my mother for the absolute support in everything. For the talks, for the patience, for the sacrifices. I only wish to make of her a proud mother. To my brother and my sister, mostly for being there. I hope to one day become an example for her and to be as good as him. I feel truly blessed and happy for this family, could not ask for a different one.



## ABSTRACT

---

This work intends to utilize a miniaturized data acquisition board, with wireless communication, to modernize labs of introductory physics classes, namely in Mechanics, Thermodynamics, and Electromagnetism, as well as to develop low cost solutions for these labs. The acquisition board used was BITalino, developed by the company PLUX. The selected experiments were the real pendulum and the Faraday induction. The real pendulum experiment uses a built-in accelerometer, while for the Faraday Induction a pre-amplifier was built in order to measure and recorded the induced voltage. A digital thermometer was also built, with the intent of being used in Thermodynamics experiments. The design philosophy of this project is to use, as much as possible, off the shelf components - both electronic and physical.

The real pendulum experiment proved a success, it allowed finding of the damping time constant of the motion, as well as how the period of a real pendulum depends on the angle of oscillation. The pre-amplifier built to measure induced voltage in  $10 - 300 \mu V$  range and the digital thermometer were tested and both showed good results.

**Keywords:** Didactic; BITalino; Pendulum; Induction; Thermodynamics; Accelerometer; Instrumentation; Do-it-yourself.

---



## RESUMO

---

Este trabalho tem por intenção desenvolver a utilização de placas de aquisição de dados miniaturizadas, com comunicação sem fios, de maneira a modernizar os laboratórios das aulas práticas de Física, nomeadamente de Mecânica, Termodinâmica e Eletromagnetismo, com soluções de baixo custo. A placa de aquisição utilizada foi um BITalino, desenvolvida pela empresa PLUX. As experiências selecionadas foram o pêndulo real e a indução de Faraday. A experiência do pêndulo real utiliza um acelerómetro montado de origem no BITalino, enquanto a experiência de indução de Faraday necessita de um pré-amplificador para medir a diferença de potencial induzida. Foi também construído um termómetro digital com o intuito de ser usado em experiências de Termodinâmica. A filosofia deste projeto é uma de faça-você-mesmo, utilizando, quando possível, materiais facilmente acessíveis.

A experiência do pêndulo real permite mostrar como se pode determinar a constante de tempo do amortecimento do pêndulo, bem como a relação entre o período de oscilação do pêndulo e o ângulo da oscilação. O pré-amplificador, construído para medir tensão induzida na gama  $10 - 300 \mu V$ , e o termómetro digital foram testados e ambos mostraram bons resultados.

**Palavras-chave:** Didático; BITalino; Pêndulo; Indução; Termodinâmica; Acelerómetro; Instrumentação; Faça-você-mesmo.

---





# CONTENTS

<b>List of Figures</b>	<b>xv</b>
<b>List of Tables</b>	<b>xix</b>
<b>1 Introduction</b>	<b>1</b>
1.1 Motivation . . . . .	1
1.2 Goals . . . . .	2
1.3 Outline . . . . .	2
<b>2 Contextualization</b>	<b>3</b>
2.1 Didactic Physics Labs . . . . .	3
2.2 BITalino . . . . .	4
2.3 Physics Labs at FCT/UNL . . . . .	5
2.3.1 Mechanics . . . . .	6
2.3.2 Electromagnetism . . . . .	7
<b>3 Pendulum</b>	<b>9</b>
3.1 Theoretical Formulations . . . . .	9
3.1.1 Acceleration of an Ideal Pendulum . . . . .	9
3.1.2 Acceleration of a Real Pendulum . . . . .	11
3.1.3 Period of a Real Pendulum . . . . .	12
3.2 Experimental Setup . . . . .	13
3.2.1 The Pendulum System . . . . .	13
3.2.2 Python Program: Pendulum Data . . . . .	14
3.2.3 Python Program: Graphical Interface . . . . .	17
3.2.4 Laboratory Guide . . . . .	17
3.3 Results and Discussion . . . . .	18
3.3.1 Results . . . . .	18
3.3.2 Finding $\tau$ . . . . .	21
3.3.3 Period of a Real Pendulum . . . . .	22
<b>4 Faraday Induction: Measuring Microvolts with BITalino</b>	<b>27</b>
4.1 Theoretical Formulations . . . . .	27

## CONTENTS

---

4.2	Experimental Setup . . . . .	28
4.2.1	System Summary . . . . .	28
4.2.2	Circuit Dimensioning . . . . .	30
4.2.3	Filter Optimization: Cutoff Frequency Effect . . . . .	31
4.2.4	Python Program . . . . .	32
4.3	Results and Discussion . . . . .	33
<b>5</b>	<b>Measuring Temperature with BITalino</b>	<b>39</b>
5.1	Experimental Setup . . . . .	39
5.1.1	Circuit Dimensioning . . . . .	39
5.1.2	Python Program: GUI . . . . .	42
5.2	Results and Discussion . . . . .	43
5.2.1	Thermometer for [263;383] K range . . . . .	43
5.2.2	Thermometer for [70;300] K range . . . . .	45
<b>6</b>	<b>Conclusion</b>	<b>47</b>
6.1	Final Remarks . . . . .	47
6.2	Future Work . . . . .	48
	<b>Bibliography</b>	<b>51</b>
<b>I</b>	<b>Annex 1 BITalino Plugged Datasheet</b>	<b>53</b>
<b>II</b>	<b>Annex 2 Accelerometer Datasheet</b>	<b>57</b>
<b>III</b>	<b>Annex 3 How to Calibrate BITalino's Accelerometer</b>	<b>59</b>
<b>IV</b>	<b>Annex 4 Real Pendulum Laboratory Guide</b>	<b>61</b>

## LIST OF FIGURES

2.1	The BITalino plugged hardware configuration 2.1a, adapted from [10]. The board mounted on a 3D printed case 2.1b. . . . .	4
3.1	A pendulum representation. . . . .	10
3.2	Representation of radial component of the gravitational acceleration and centripetal acceleration. . . . .	11
3.3	Comparison of theoretical radial acceleration and angle of oscillation. Angle calculated with equation 3.8. Acceleration calculated with equation 3.9. With these conditions: $r = 16\text{ m}$ , $\omega = 0.7826\text{ rad} \cdot \text{s}^{-1}$ , $\theta_0 = 45^\circ$ and $\tau = 45\text{ s}$ . . . . .	13
3.4	The projected pendulum system. Thought out to be a build-it-yourself system using off the shelf materials, while maintaining stability for a good oscillation. 1 oscillating mass; 2 BITalino attached to the mass; 3 strings; 4 supports for the rods; 5 pivot rod; 6 metal rods for support. . . . .	14
3.5	Real pendulum experiment setup. BITalino attached to the oscillating mass. . . . .	15
3.6	Diagram of measuring radial acceleration on BITalino's z axis. BITalino's three axis are drawn in white. . . . .	15
3.7	The radial acceleration of an oscillating 0.600 kg mass with a length of oscillation $r$ of 0.3m. . . . .	16
3.8	Detail of calculated minima and maxima. . . . .	17
3.9	The pendulum experiment GUI. For a complete rundown of all the buttons and functionalities see Annex . . . . .	18
3.10	The radial acceleration of an oscillating 0.600 kg mass with a length of oscillation $r$ of 0.3 m. The starting angle was $\theta_0 = 65^\circ$ . In red, the local maxima of acceleration and in yellow the local minima. . . . .	19
3.11	MEMS accelerometer diagram. . . . .	19
3.12	z axis accelerometer behavior when the BITalino is stationary in three different positions: a) BITalino is perpendicular to the resting position, in our pendulum system this is equivalent to a $90^\circ$ angle; b) upside down BITalino; c) the resting position used for our measurements . . . . .	20
3.13	This is the type that is expected of the students to find. Two lines with acquired maxima and minima. And two lines where the student must find the $\tau$ that better fits the experimental data. In this graph $\tau = 115\text{ s}$ . . . . .	20

3.14	Variation of the damping time versus the mass of the pendulum. Note that the proportionality $\tau \propto m$ expected for viscous damping is not verified. . . . .	21
3.15	Angle of oscillation of a pendulum with $r = 0.32 m$ , $m = 0.600 kg$ . In blues the angle calculated using the minima of acceleration. In red the angles calculated using the maxima of acceleration. In black the theoretical curve. . . . .	22
3.16	Evolution of the period of one oscillation throughout the pendulum motion. In blue dots the period of every oscillation, in red the average for 5 consecutive periods. The period of one oscillation is decreases with amplitude oscillation. . . . .	23
3.17	Period in seconds versus angle of oscillation in degrees. In blue, the raw data and, in red, the averaged over 5 consecutive points data. Note the non-linear increase of the period for greater angles. . . . .	23
3.18	$\varepsilon$ in function of the squared angle. Plot made with the average of 5 consecutive angles and time periods. . . . .	24
3.19	$\varepsilon$ in function of the squared angle. Plot made with the average of 5 consecutive angles and time periods. In blue $m = 0.600 kg$ ; in yellow $m = 0.400 kg$ ; in red $m = 0.200 kg$ . . . . .	25
4.1	Conductive ring in a static magnetic field . . . . .	28
4.2	Diagram of the experimental system. (1) is the induction system. (2) is an electric rotor. (3) is a voltmeter. . . . .	29
4.3	Faraday induction experimental setup. . . . .	29
4.4	A two stage amplifier, for a total of 5151 gain, with a low-pass 1 Hz filter to reduce noise. . . . .	30
4.5	The pre-amplifier assembled on a box. Banana connectors to connect to the wire loops and a USB connector to connect the amplifier to BITalino. . . . .	31
4.6	Cutoff frequency response to different load resistances. Higher resistance means the filter takes longer to act. . . . .	32
4.7	Typical plot of induced tension in function of time. . . . .	33
4.8	The Faraday induction experiment GUI. . . . .	33
4.9	Voltage induced, at constant speed and constant magnetic field intensity, on a loop of varying widths: in red, a width of $0.040 m$ ; in blue width of $0.028 m$ ; and in yellow width of $0.02.0 m$ . As predicted the voltage at width $0.040 m$ is double the voltage induced on a loop of $0.02.0 m$ width. . . . .	34
4.10	Voltage induced on a loop of constant width, moving through a static magnetic field at different velocities: in red, $v = 0.020 m/s^{-2}$ ; in blue $v = 0.040 m/s^{-2}$ ; and in yellow $v = 0.080 m/s^{-2}$ . . . . .	35
4.11	Voltage induced on a loop of constant width, moving, at constant velocity, through a static magnetic field, with varying intensities. . . . .	35
4.12	Plot of averaged $\varepsilon$ in function of $b$ . With a linear fit equation. . . . .	36
4.13	Plot of averaged $\varepsilon$ in function of $v$ . With a linear fit equation. . . . .	37
4.14	Plot of averaged $\varepsilon$ in function of number of magnets. With a linear fit equation. . . . .	37

---

5.1	Wheatstone bridge. $R_x$ is where the Pt100 is connected. $R_3$ is the reference resistance. . . . .	40
5.2	Circuit schematic for temperature measurement with a Pt100 and a BITalino.	41
5.3	The effect of saturation of the LM 358 in red, as measured with a reference resistance $R_2 = 93.2 \Omega$ and a gain of 10. In blue the output of an ideal operational amplifier, for a circuit with the same reference resistance and gain. . .	42
5.4	The thermometer GUI. . . . .	43
5.5	Measured and theoretical temperatures in function of test resistances. . . . .	44
5.6	In blue the difference between measured and expected temperature, $\Delta T = T_m - T_e$ , in function of the Temperature. In black the gain of the circuit. . . .	45
5.7	Measured and theoretical temperatures in function of test resistances. . . . .	46
5.8	In blue the difference between measured and expected temperature, $\Delta T = T_m - T_e$ , in function of the Temperature. In black the gain of the circuit. . . .	46
III.1	Accelerometer calibration movement. . . . .	60
III.2	Accelerometer calibrationn data in bits in gray. In blue the smoothed data. .	60



## LIST OF TABLES

2.1	BITalino plugged specifications, with an accelerometer installed. . . . .	5
2.2	Sensors used in Mechanics experiments. . . . .	7
2.3	Measurement equipment for Electromagnetism labs. . . . .	8
3.1	$\tau$ found for pendulum length $r = 0.32\text{ m}$ . . . . .	21
3.2	Linear fit equations for masses with pendulum length $r = 0.32\text{ m}$ . . . . .	24
4.1	Cutoff frequency for different resistances. . . . .	31
4.2	Results obtained for $v = 0.067\text{ m/s}$ and 8 pairs of magnets, with varying loop width. . . . .	34
4.3	Results obtained for 8 pairs of magnets and $b = 0.04\text{ m}$ , with varying velocity. . . . .	34
4.4	Results obtained for $v = 0.086\text{ m/s}$ and $b = 0.04\text{ m}$ , with varying magnetic field intensity. . . . .	35
5.1	Theoretical bridge voltage for the two reference resistances used in section 5.2. . . . .	41
5.2	Measurement ranges and respective resolutions. . . . .	41
5.3	Practical measurement ranges and respective resolutions. . . . .	42





## INTRODUCTION

### 1.1 Motivation

There have been great developments in both miniaturization of signal acquisition equipment and wireless data transmission. As these technologies become more accessible and affordable, they open new possibilities in many areas. One such area is the development of didactic material for physics labs.

Generally, the material required for experiments in introductory physics (Mechanics, Thermodynamics, and Electromagnetism) is sold by a handful of companies, such as LeyBold, Pasco, and Phywe. But this material has become costly. There is also a glaring compatibility problem, as components from one provider are usually not compatible with materials from another provider.

In this context, the goal of this thesis is to utilize new advancements in technology to develop new experiments and adapt old ones, while providing a lower cost and open source alternative to the commercially available didactic equipment. For this purpose, a partnership with PLUX, a Portuguese company that specializes in biomedical equipment for education and research applications, has been established. In the context of this thesis, PLUX provides access to equipment and technical support. The equipment provided is BITalino, a low-cost toolkit that has the required signal acquisition and wireless data transmission capabilities that is relatively inexpensive.

We used BITalino in two experiments. The first experiment is a study of the motion of a pendulum. This was the model experiment of this work, it emphasizes new possibilities of experiments making use of the accelerometer installed on BITalino. The second experiment is about the Faraday induction. In this experiment the focus is on the adaptability and the do-it-yourself mindset of the BITalino, additional circuitry was developed to function as micro-voltmeter. Further building upon this mindset, BITalino is also used

to measure temperature with a Pt100 resistance temperature detector.

## 1.2 Goals

The first goal of this project was to create a simple Graphical User Interface (GUI), in which a user can visualize the acquired data in real-time during the experiment. Another key aspect of using automatic data recording to enable the student to use a standard Excel worksheet for data analysis. Secondly it was determined which experiments, of those currently performed in labs of introductory physics courses, could best serve to exemplify BITalino's didactic capabilities. Given that a great number of experiments can be done, it was decided to focus on two experiments. One can fully utilize the new acquisition board, the other takes advantage of the computerized acquisition system to further enhance the students' access to information. The chosen experiments were: the study of the pendulum motion, and a Faraday induction study. A case study for making temperature measurements using a Pt100 resistance temperature detector and a BITalino, was performed.

## 1.3 Outline

In the present chapter the problem, motivation and overall goals of the work are introduced.

Chapter 2 explains why the pendulum and the Faraday induction experiments were chosen, as well as a review of the most relevant commercially available solutions for these experiments. Also in this chapter, the BITalino board is introduced, with an overview of its technical properties.

Chapter 3 first introduces how an acceleration measurement system with wireless capabilities brings forth new possibilities for the study of pendulum motion. It then proceeds to detail the experimental setup developed. To conclude it shows the acquired data, and how they compare with the elementary theory.

Chapter 4 introduces relevant concepts regarding how the Faraday induction experiment is performed, and how using the BITalino makes it more visually appealing, and lowers the cost. The chapter then proceeds to show how off-the-shelf components can be used to build a 'homemade' microvoltmeter. To conclude, experimental results show the feasibility of our solution using the BITalino and our 'homemade' microvoltmeter.

Chapter 5 is a case study of how a simple circuit with a Pt100 and a BITalino could be used as temperature measurement equipment.

Finally, Chapter 6 outlines the main conclusions of this work, and provides insights for future development.

## CONTEXTUALIZATION

This chapter presents an overview of the state-of-the-art on existing tools for physics didactic experiments. Secondly, the choice of the BITalino acquisition board is justified, presenting relevant technical characteristics. Finally, an overview of the experiments done on introductory physics labs at FCT/UNL.

### 2.1 Didactic Physics Labs

Lab experiments are a key part of learning physics. Some studies suggest that they help with retention ability [1], foster critical-thinking abilities [2], and teach students to test and evaluate models [3]. The use of hands-on lab experiments for increasing student performance is still up for debate, however [4] suggests it does not systematically increase students performances on final exams.

As an alternative to hands-on labs, there are simulation based labs. Recent studies suggest that students learn equally well from either type of experience [5]. In the same study it was found that the biggest difference between hands-on and simulation labs is in the perception of the students. While the conclusions cannot be generalized, students in this study felt they learn better from hands-on experiences.

However, lab experiments, either hands-on or simulation, are still widely used. Almost every undergraduate, as well as high school, level physics class features lab assignments in which the students are expected to apply knowledge, acquired in theoretical classes, to a practical example. A market exists to facilitate access to equipment for these labs, and, as technology evolves, so must the experiences.

Many didactic experiment kits now come with signal acquisition boards, and a computer interface to visualize the data. PASCO Scientific has the 550 Universal Interface, Leybold features the Sensor-CASSY 2, Phywe sells the Cobra4 Xpert-Link, etc. For each

of the acquisition boards mentioned before, there is a corresponding program to control the board, and visualize data. Each interface only works with sensors of their respective brand.

Developments in both miniaturization of signal acquisition equipment and wireless data transmission open new possibilities in many areas. PLUX has developed BITalino, which is a low-cost toolkit to learn and prototype applications using body signals [6]. This new facet of acquisition boards comes about from a global revolution in the way the physical and the digital world interact, which, itself, is closely related to the 'do-it-yourself' movement. The popularity of Arduino and Raspberry Pi are proof of this [7]. An example of the do-it-yourself mentality is the Creator Kit from Fritzing company [8], which provides an introduction to do-it-yourself electronics. Another similar kit is the Sparkfun Inventor's Kit - V3.3 which provides basic electronic components for \$100 [9].

## 2.2 BITalino

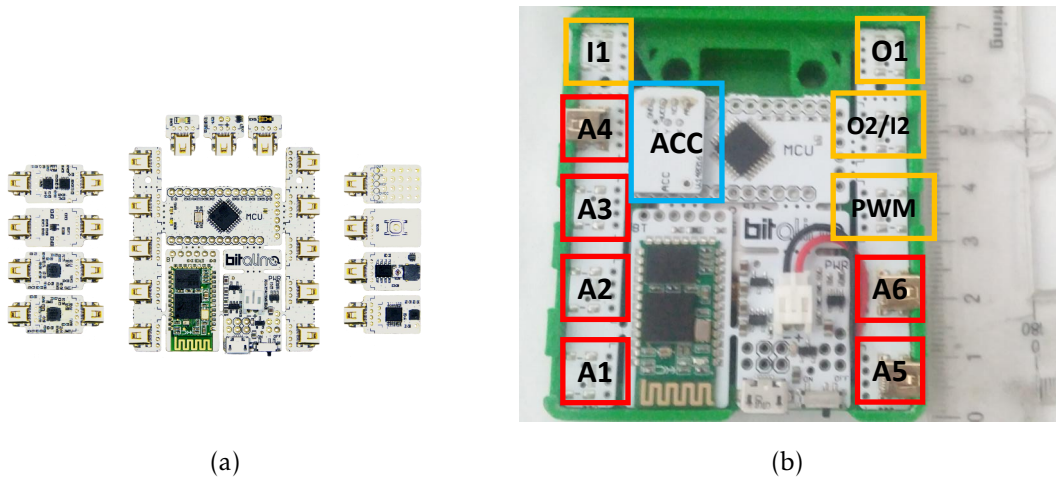


Figure 2.1: The BITalino plugged hardware configuration 2.1a, adapted from [10]. The board mounted on a 3D printed case 2.1b.

PLUX has commercialized its low-cost (starting at 149€ + shipping) acquisition board BITalino since August 2013. BITalino's low-cost was thought out as a community motivator, it was not designed to be a money-maker [11]. The hardware consists of a low cost, modular wireless biosignal acquisition system with a credit card-sized form factor. The motivation behind using BITalino comes from these three conditions. The wireless acquisition system is an interesting concept that might prove to be useful in developing new experiments, namely in Mechanics experiments. The small dimensions of the system and the wireless acquisition system allow for implementation in a greater number of experiments. Additionally, BITalino has a whole set of available software tools that lets a greater number of people just pick it up and start developing new things. All this for an affordable price make BITalino an excellent choice for the project we are developing.

BITalino has three different configurations available for purchase, *Board, Plugged, and Freestyle* [6, 12]. Figure 2.1b displays the plugged configuration used on our work. In this configuration plugs are added to BITalino's ports. Table 2.1 presents the specifications of the individual blocks, provided by default on the analog front-end. BITalino was designed to have a set of generic analogue ports, in this way it is possible to connect sensors with analog outputs. Moreover, it is possible to develop specific sensors for many applications, and connect them to BITalino.

Table 2.1: BITalino plugged specifications, with an accelerometer installed.

Specifications	
Sampling Rate	Configurable to 1, 10, 100, 1000 Hz
Analog Ports	4 input (10 bit) + 2 input(6 bit)
Digital Ports	1 input (1 bit) + 4 output(1 bit)
Data link	Class II Bluetooth v2.0 ( 10 m range)
Actuators	LED
Sensors	Tri-axial accelerometer
Weight	30 g
Size	100 x 60 mm
Battery	3.7 V LiPo
Consumption	65 mAh (with all peripherals active)

The ports enumerated in table 2.1 are identified on the board as per figure 2.1b. Ports **I1**, **O2**, and **I2/O2** are digital input and output ports. **PWM** is a pulse width modulator, usually used to control a digital-analog converter. Ports **A1-A6** are the analog ports, of which **A5** and **A6** are 6 bit input ports and the others are 10 bit input ports. On the board used in this work, we connected a tri-axial accelerometer (**ACC** to ports **A1**, **A2**, and **A3** (one port for each axis of measurement) as can be seen in figure 2.1b. We used the 10 bit analog port **A4** to connect different sensors.

BITalino has several application programming interfaces (API) that allow to easily incorporate BITalino in custom made software applications. In the context of this work we used the Python API.

## 2.3 Physics Labs at FCT/UNL

Whether developing new or adapting old experiences, we are looking to make better and/or more affordable experiments. In this context, why is the pendulum the model experiment of this work? Why choose an experiment on Faraday induction over other experiments concerning electromagnetism? To help answer these questions a review of the available experiments at FCT/UNL is made.

### 2.3.1 Mechanics

The FCT/UNL Mechanics laboratory class of the Physics Department is equipped to perform a total of 13 experiments:

1. Average velocity;
2. Newton's 2nd law;
3. Projectile motion;
4. Angular momentum;
5. One dimensional collisions;
6. Two dimensional elastic collisions;
7. Rotational collisions;
8. Centrifugal force;
9. Simple Pendulum;
10. Compound pendulum;
11. Ballistic pendulum;
12. Non isochronous pendulum;
13. Ideal spring.

In table 2.2 the necessary sensors for each of these experiments are enumerated. In the far right column it is also indicated if the acquired data are immediately sent to a computer.

All these experiments use PASCO Scientific equipment and software (DataStudio). This equipment was bought a few years ago, since then PASCO has updated its catalog, introducing new equipment and discontinuing some of its old equipment. PASCO also developed a new interface software, PASCO Capstone, and stopped updating their previous DataStudio software [13]. This means new hardware does not work with old software. For instance, the PASPORT Motion Sensor PS-2103A requires the PASCO 850 Universal Interface in order to visualize the data [14]. The 850 Universal Interface, however, does not work with the old DataStudio software and requires PASCO Capstone software [15]. This reveals another advantage of using open source equipment. Anyone with the necessary expertise can adapt what has been done before to their own needs.

Experiments that require a sonar sensor are usually interested in tracking the position of an object, as is the case of the one dimensional collisions experiment. With just an accelerometer it is not possible to know the exact position of the BITalino. It is, however, possible to know at what point in time did the moving object changes direction, due to a

Table 2.2: Sensors used in Mechanics experiments.

	Motion Sensor	Timer	Photogates	Sonar	Computer
Average velocity	-	1	-	2	-
Newton's 2nd law	-	-	-	1	✓
Projectile Motion	-	-	-	-	-
Angular momentum	-	1	1	-	-
One dimensional collision	-	2	2	2	✓
Two dimensional collision	-	-	-	-	-
Rotational collision	1	-	-	-	✓
Centrifugal force	-	1	-	-	-
Simple Pendulum	-	1	-	1	-
Compound pendulum	-	-	1	1	-
Ballistic pendulum	-	1	2	-	-
Non isochronous pendulum	1	-	-	-	✓
Ideal Spring	-	-	-	1	✓
<b>Total</b>	<b>3</b>	<b>5</b>	<b>5</b>	<b>9</b>	

collision for instance, through a measurement in acceleration. It might then be possible to adapt this experiment to work with acceleration measurements.

In Mechanics experiments, one advantage of the BITalino with an accelerometer equipped is in fact the wireless data transmission capability, which makes it possible to attach the board to a moving object and record data with no topological drawbacks from attached wires. This is the case for pendulum based experiments, this being the main reason why the real pendulum experiment is the model experiment in this work.

The simple and compound pendulum experiments performed are not quite up to par with the richness of this system. They consist of using a timer and a photogate to measure the period of one pendulum oscillation. The period is then used to determine free fall acceleration on the surface of the Earth,  $g$ . However, a pendulum experiment can be used for more. For instance, to study harmonic oscillation, and to study the effect of damping. By attaching the BITalino to the oscillating mass and measuring the acceleration, we propose that a new pendulum experiment that can be designed to more extensively study its motion. At the same time, this makes the experimental setup much simpler, as will be described in chapter 3.

### 2.3.2 Electromagnetism

The FCT/UNL Electromagnetism lab is equipped to perform a total of 6 experiments:

1. The oscilloscope;
2. Tracing electric field equipotential lines;
3. Ohm's law and DC circuits;

4. Charge and discharge of capacitors;
5. Electron trajectories in a magnetic field;
6. Faraday induction 1, conductive ring moving through a magnetic field;
7. Faraday induction 2, magnetic flux variations by means of a coil;

In table 2.3 the necessary measurement equipment is enumerated.

Table 2.3: Measurement equipment for Electromagnetism labs.

	Voltmeter	Ammeter	Oscilloscope	Timer	Computer
Oscilloscope	-	-	1	-	-
Equipotential lines	1	-	-	-	-
DC circuits	1	1	-	-	-
Capacitor	-	-	1	-	-
Electron trajectories	-	-	-	-	-
Faraday induction 1	1	-	-	1	-
Faraday induction 2	1	1	-	-	-
<b>Total</b>	<b>4</b>	<b>2</b>	<b>2</b>	<b>1</b>	

Some of these experiments are inherently made to be used with certain equipment. The oscilloscope experiment's goal is to familiarize the student with the oscilloscope functionalities. It is therefore absolutely necessary to use the oscilloscope. The equipotential lines are supposed to be drawn on paper by the student. The electron trajectories experiment is the experiment that requires the most material, but the students are only requested to measure diameters of circular trajectories versus magnetic field and acceleration potential.

The remaining experiments could have their measurement tools replaced by a BITalino. However, BITalino has a few limitations that, at this time, make some of these experiments difficult to adapt. These experiments are the capacitors experiment and the Faraday induction 2. They concern phenomena that happen in a frequency range higher than BITalino's highest sampling rate (1000 Hz). The charge frequency on the RC circuits tested is on the order of kHz, and the frequency of the Faraday induction experiment is in the 100 – 2000 Hz range.

Thus, we chose the Faraday induction 1 experiment because this experiment needs to measure microvolts and it does not have the limitations mentioned above. The BITalino does not have the necessary resolution to measure voltage in the order of microvolts, for this reason a pre-amplifier must be built, giving the chance to embrace the do-it-yourself mentality. Applying the BITalino to this experiment also makes a few other improvements regarding data visualization, as will be discussed in chapter 4.



## PENDULUM

In this chapter the pendulum experiment will be described. Firstly, a theoretical contextualization is made in section 3.1. This experiment has two objectives. The first objective is to experimentally determine the damping time constant,  $\tau$ , of a real pendulum. The second objective is to demonstrate that for a real pendulum the oscillation period depends on the angle.

Secondly, the experimental setup is presented in section 3.2. What is new about our experiment design is that the BITalino with an equipped accelerometer is part of the oscillating body. The board itself can oscillate because there are no wires to connect the accelerometer to the acquisition board. With this setup the measured quantity is acceleration. However, thinking in terms of acceleration is not intuitive: our mind is more trained to analyze position or velocity variations than acceleration variations.

In section 3.3 results and discussion are presented. The acquired acceleration data are plotted and compared to theoretical data. It is shown how, utilizing, the acquired data it is possible to achieve the proposed goals of the experiment.

### 3.1 Theoretical Formulations

#### 3.1.1 Acceleration of an Ideal Pendulum

The pendulum is an example of a non-uniform circular motion. It consists of an object of mass  $m$  attached to the end of a string of length  $r$ . The other end of the string is attached to stationary point.  $\theta$  is the angular position of the object, with respect to the downward vertical, see figure 3.1. If damping forces are neglected, it can be deduced that the differential equation 3.1 describes the motion of a simple pendulum.

$$\frac{d^2\theta}{dt^2} + \frac{g}{r} \sin \theta = 0 \quad (3.1)$$

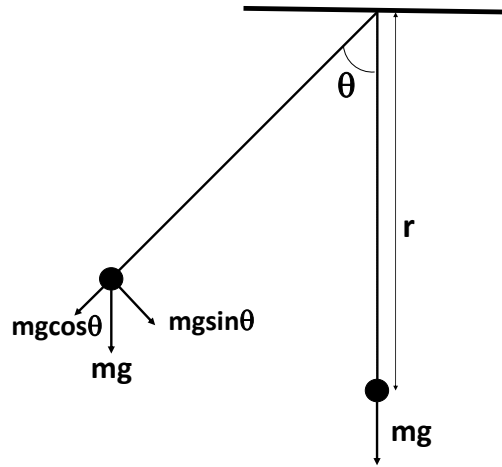


Figure 3.1: A pendulum representation.

in which  $g$  is the gravitational acceleration. Making use of the small angle approximation,  $\sin \theta \approx \theta$ , expression 3.1 becomes the expression for the angular movement of an ideal pendulum:

$$\frac{d^2\theta}{dt^2} + \frac{g}{r}\theta = 0 \quad (3.2)$$

equation 3.2 is the differential equation for a simple oscillatory movement with angular frequency  $\omega = \sqrt{\frac{g}{r}}$ . A possible solution for this equation is:

$$\theta(t) = \theta_0 \cos(\omega t + \phi) \quad (3.3)$$

$\phi$  is the initial phase of the movement,  $\theta_0$  is the amplitude of the movement.  $\phi$  and  $\theta_0$  are initial conditions of the movement. For simplicity's sake, we will consider  $\phi = 0$ : this condition implies that the pendulum is dropped from its maximum amplitude at  $t = 0$ .

Thus,  $\theta(t) = \theta_0 \cos(\omega t)$  is the equation that describes the angular motion for a small angle ideal pendulum. It follows that the pendulum has radial,  $v_r$ , and tangential,  $v_\theta$ , velocities given by:

$$v_r = \dot{r} \quad (3.4)$$

$$v_\theta = r\dot{\theta} \quad (3.5)$$

because  $r$  is constant,  $v_r = 0$ . The radial (or centripetal) and tangential acceleration are, respectively, given by:

$$a_r = \frac{v_\theta^2}{r} \quad (3.6)$$

$$a_\theta = r\dot{v}_\theta \quad (3.7)$$

### 3.1.2 Acceleration of a Real Pendulum

The first objective of this experiment is to determine the damping time constant of a real pendulum. Introducing viscous damping to equation 3.2 makes it so the amplitude of movement decreases exponentially. A solution to this equation can be:

$$\theta(t) = \theta_0 \cos(\omega t) \exp(-t/\tau) \quad (3.8)$$

replacing 3.8 in eq. 3.6, we get the radial acceleration given by 3.9:

$$a_r = r\theta_0^2 \exp^{-2t/\tau} \left[ \omega \sin(\omega t) + \frac{\cos(\omega t)}{\tau} \right]^2 \quad (3.9)$$

thinking in terms of acceleration is not common and usually not very intuitive. At the position where the tangential velocity is zero, the centripetal acceleration of the pendulum given by  $\frac{v_\theta^2}{r}$  is also zero, as seen in figure 3.2 Therefore, at this point the force along the radial axis should be less than when the pendulum passes through its resting position, where the centripetal acceleration is at its maximum. Thus, there is a radial acceleration maximum whenever the pendulum passes the position where  $\theta = 0$ . Because, during a full oscillation, the pendulum crosses this point twice, there are two maxima of acceleration for each pendulum oscillation. The same happens for minima of acceleration. This reasoning implies that the frequency of the radial acceleration is twice that of the angle. Mathematically, this frequency doubling comes from the fact that this acceleration is calculated as the square of an harmonic oscillation, as shown in equation 3.9.

To the acceleration caused by the gravitational force we must add the centripetal acceleration of a circular motion. In figure 3.2 we see that the centripetal acceleration is null when the pendulum reaches its maximum angle. The centripetal acceleration is always zero when the object is stationary. When the pendulum crosses  $\theta = 0$  the centripetal acceleration is maxed.

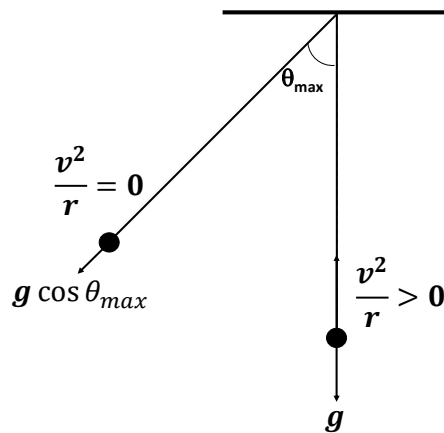


Figure 3.2: Representation of radial component of the gravitational acceleration and centripetal acceleration.

In the case of low damping, the radial acceleration can be calculated for the two extreme cases where  $\omega t = n\pi$  and  $\omega t = n\pi + \pi/2$ .

For  $\omega t = n\pi$  :

$$\sin(n\pi) = 0 \quad \cos(n\pi) = \pm 1 \quad (3.10)$$

$$a_r = \frac{r\theta_0^2}{\tau^2} \exp(-2t/\tau) \quad (3.11)$$

for  $\omega t = n\pi + \pi/2$  :

$$\sin(n\pi + \pi/2) = \pm 1 \quad \cos(n\pi + \pi/2) = 0 \quad (3.12)$$

$$a_r = r\theta_0^2\omega^2 \exp(-2t/\tau) \quad (3.13)$$

at the same time, replacing  $\omega t = n\pi \vee \omega t = n\pi + \pi/2$  on equation 3.8 it results in:

$$\theta(n\pi) = \theta_0 \cos(n\pi) \exp^{-t/\tau} = \pm \theta_{max} \quad (3.14)$$

$$\theta(n\pi + \pi/2) = \theta_0 \cos(n\pi + \pi/2) \exp^{-t/\tau} = 0 \quad (3.15)$$

the radial component of the gravitation force is maximized when the pendulum is at  $\theta = 0$ , thus the radial acceleration is maxed at this angle. Figure 3.3 shows the relationship between angle and radial acceleration.

We can now say that to find  $\tau$  we only need to know  $r$ ,  $\omega$ ,  $\theta_0$  and the maxima of radial acceleration. We expect these maxima to vary with  $\exp(-2t/\tau)$ . Therefore, if a plot is made of the experimental and theoretical maxima it is possible to adjust  $\tau$  on the theoretical data so that it matches the experimental results.

### 3.1.3 Period of a Real Pendulum

The second objective of this experiment is to verify that the period of oscillation of a real pendulum depends on the angle of oscillation if the condition  $\theta \ll 1$  is not verified. In this case, the period of a pendulum can be approximated by:

$$T = 2\pi \sqrt{\frac{r}{g}} \left[ 1 + \frac{1}{16} \theta_0^2 + \frac{1}{3072} \theta_0^4 + \dots \right] \quad (3.16)$$

in this expression it is also possible to see the small angle approximation, if  $\theta \ll 1$  the latter contributions of the series are negligible. These latter contributions can be considered corrections to the small angle approximation. So,  $T_0 = 2\pi \sqrt{\frac{r}{g}}$  is the small angle approximation, adding  $T_1 = T_0 \cdot \frac{1}{16} \theta_0^2$  would be a first correction to the approximation, and so on with the following terms of the series.

In this context, the objective will be to measure the period of oscillation from the measured acceleration and show:

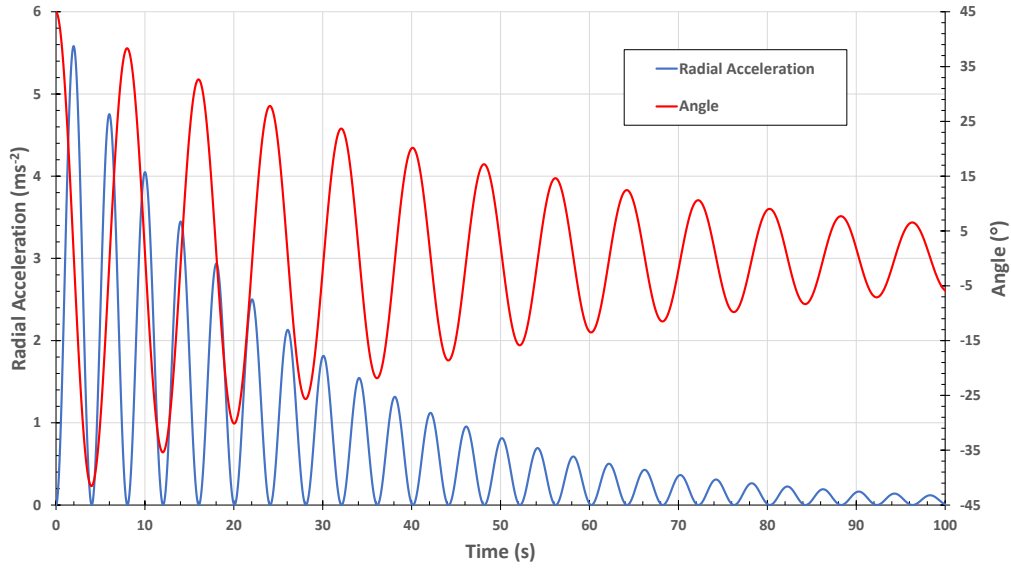


Figure 3.3: Comparison of theoretical radial acceleration and angle of oscillation. Angle calculated with equation 3.8. Acceleration calculated with equation 3.9. With these conditions:  $r = 16 \text{ m}$ ,  $\omega = 0.7826 \text{ rad} \cdot \text{s}^{-1}$ ,  $\theta_0 = 45^\circ$  and  $\tau = 45 \text{ s}$ .

- The period is not constant but decreases with time. Or rather, the period decreases as the amplitude decreases;
- And then show how this dependency follows equation 3.16.

## 3.2 Experimental Setup

### 3.2.1 The Pendulum System

The planned pendulum system is shown in figure 3.4. The idea here is to have an oscillating mass (1) with an attached BITalino (2). Mass (1) is attached to one end of two strings (3) suspended from a pivot rod (5). Rod (5) is secured in place by two clamps, one for each rod (6). Finally, supports (4) give stability to the entire system.

The system uses two strings to force oscillation to occur on the  $(x, z)$  plane. Ideally, with one string the oscillation starts with the mass at a  $90^\circ$  angle between axis  $x$  and  $y$ . As a matter of fact, with a pendulum using only one string, it would be very difficult to avoid oscillations in the  $y$  direction: the analysis of the motion becomes more complicated without adding any didactic information. Therefore, the mass is suspended from two strings to limit oscillations on the  $(z, y)$  plane.

Figure 3.5 shows a photograph of the built system. All the materials were re-used from spare parts of the Mechanics Laboratory of the university. Because this is a quick and cheap experimental setup there are some limitations. The available supports are not strong enough to sustain large oscillating masses, this can lead to small abnormalities

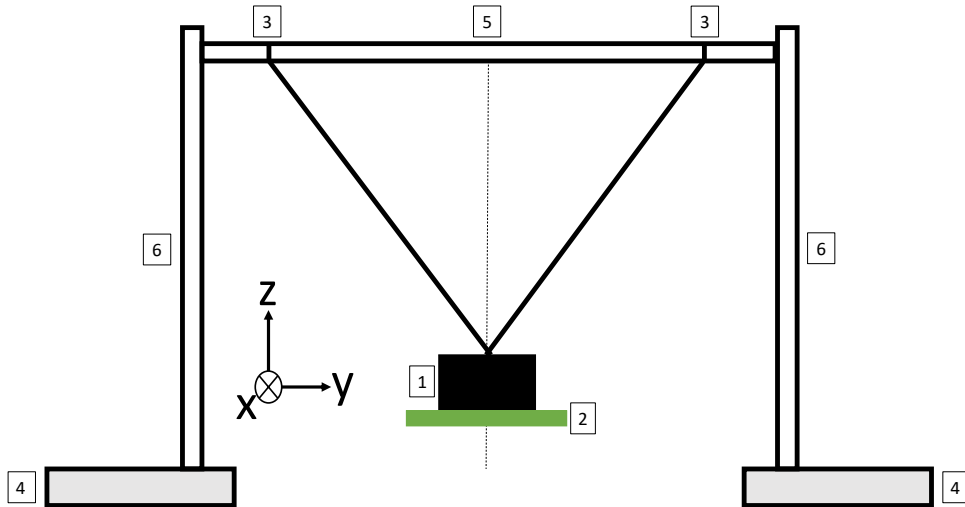


Figure 3.4: The projected pendulum system. Thought out to be a build-it-yourself system using off the shelf materials, while maintaining stability for a good oscillation. **1** oscillating mass; **2** BITalino attached to the mass; **3** strings; **4** supports for the rods; **5** pivot rod; **6** metal rods for support.

in the motion. Possible solutions would be to either use heavier supports or to fix the supports to the working station.

The strings should have the same length but because of the knots' quality it might happen that, during the oscillation of the pendulum, one of the knots gets loose and stretches. This causes the pendulum to skew to one side causing the oscillation to occur in more than two directions. Because the strings are tied to the horizontal bar, we need to make sure they do not slide across the bar during oscillation. We decided to fix them by putting tape on top of the knot and over the bar. An improvement to this issue would be to drill two holes on the horizontal bar and to pass the strings through the bar. This would also make it easier to adjust string length for different experiments.

In regards to the BITalino attachment, because it has a tri-axial accelerometer there is some flexibility as to where it can be attached. In this build, it was found best to attach the BITalino to the bottom of the mass, and so the accelerometer will measure the radial acceleration on its z-axis, see figure 3.6.

### 3.2.2 Python Program: Pendulum Data

The function that transforms digital value sampled, ADC, to acceleration in g, ACC, called a transfer function, is given in the accelerometer datasheet (Annex II):

$$ACC(g) = \frac{ADC - C_{min}}{C_{max} - C_{min}} \cdot 2 - 1 \quad (3.17)$$

where ADC is the digital value sampled, in bit.  $C_{min}$  and  $C_{max}$  are the values, in bit, corresponding to acceleration  $-1g$  and  $+1g$ , respectively. These two values can be calibrated

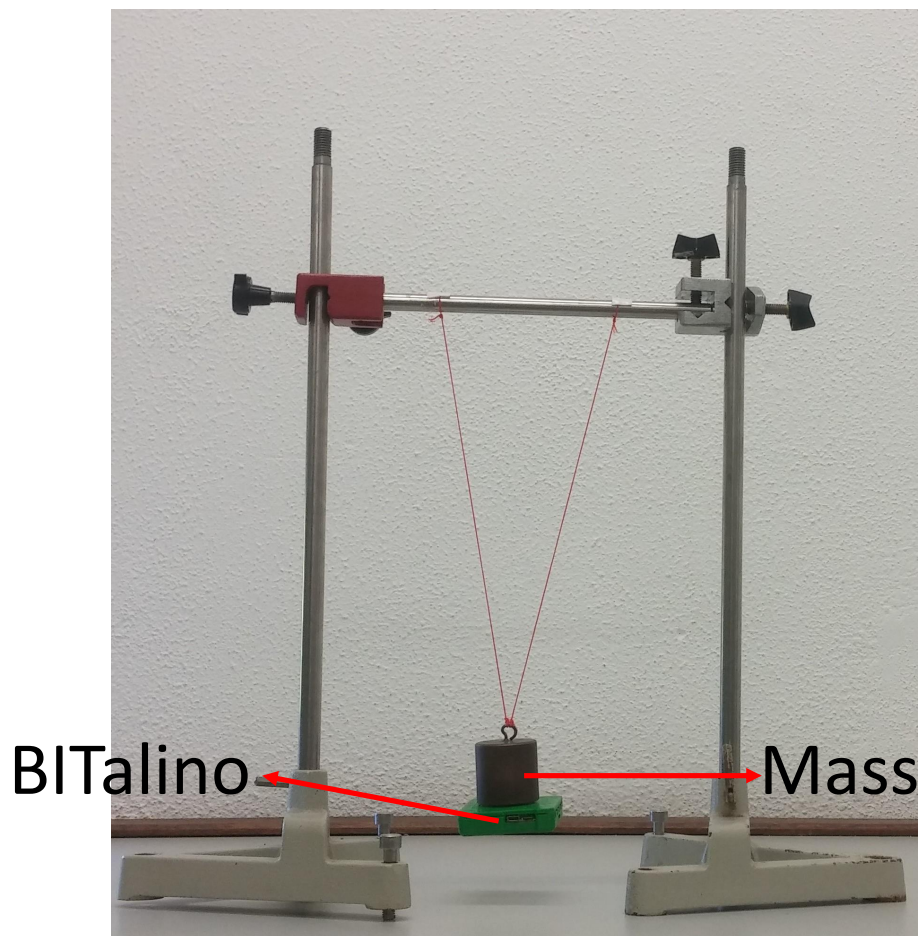


Figure 3.5: Real pendulum experiment setup. BITalino attached to the oscillating mass.

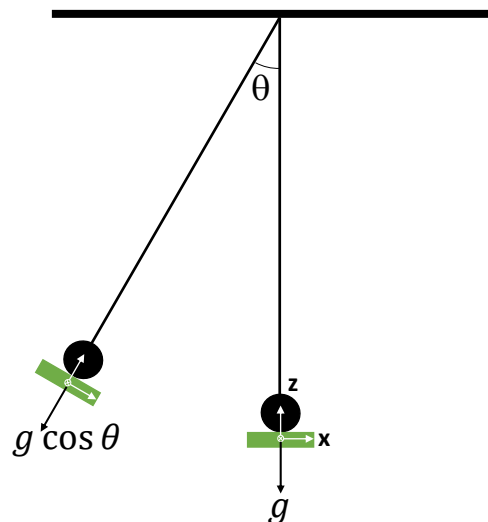


Figure 3.6: Diagram of measuring radial acceleration on BITalino's  $z$  axis. BITalino's three axes are drawn in white.

before the experiment is made. In Annex III we describe how to calibrate BITalino's accelerometer.

The resulting data from a pendulum motion are plotted using Excel to obtain figure 3.7. This data will be further discussed in section 3.3.

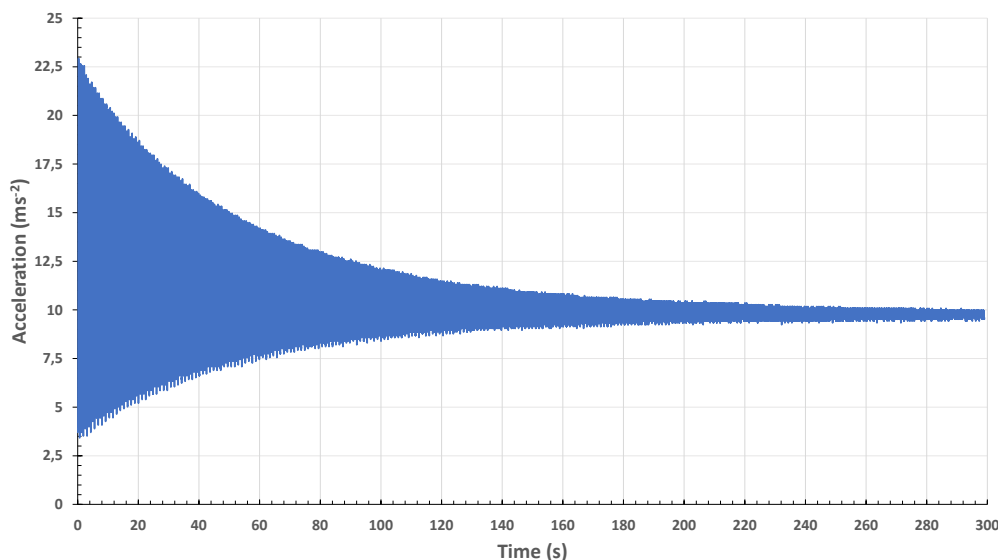


Figure 3.7: The radial acceleration of an oscillating  $0.600\text{ kg}$  mass with a length of oscillation  $r$  of  $0.3m$ .

As previously discussed, there is interest in finding the local maxima and minima of the acquired data. As this would be a relatively difficult task to give to a student in Introductory Physics, the program finds and registers these points when the data are saved.

A Python script smooths the data to facilitate peak finding. A different script then finds the points in time at which peaks occur. The time at which the smoothed maxima and minima occur is the same as in the original data. Figure 3.8 shows how the maxima and minima calculated by the script are in good agreement with the acquired data.

We have already mentioned how a period of oscillation has two maxima and two minima of acceleration. This is why, in Figure 3.8, we only mark every other maximum and minimum. This allows for the student to obtain directly in a file the value of the oscillation motion versus time without any complicated treatment. As we have seen a single acceleration period comprises two minima, corresponding to  $\pm\theta_{max}$ , and two maxima, because the oscillation crosses  $\theta = 0$  twice. This makes it easier to treat the data latter on, and it gives a fast way to calculate the period of oscillation. This figure also shows that the acceleration value is not 'equal' for two consecutive minima (beside the natural decrease due to damping). This is a consequence of an asymmetry in the pendulum system.



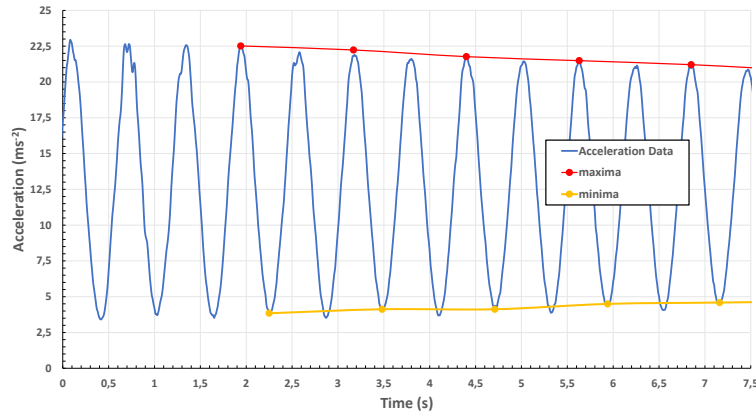


Figure 3.8: Detail of calculated minima and maxima.

### 3.2.3 Python Program: Graphical Interface

Figure 3.9 shows the graphical user interface (GUI) for the pendulum experiment. Its primary function is to show acquired data in real-time. There is also an option for calibrating the accelerometer. For the first stage of this work, the GUI was made with no concern for looks. The priority was to build a robust program that would allow for data visualization in real time.

The program has a *save* button which creates an Excel file with two sheets, as well as a text file. The first sheet has all points of acceleration acquired. The calibration values can be used, in conjunction with the raw data, to retrace the steps in finding the maxima and minima. The other has the maxima and minima, as well as corresponding time stamps. The text file has the raw data acquired by the BITalino and a header with information like: sampling rate, total acquisition time,  $C_{min}$  and  $C_{max}$ .

There are two possible ways to visualize data being acquired:

- **Window mode.** In this mode the plot will always show the data recorded during the last  $X$  seconds. The amount of  $X$  time shown is set in the **Interval (s)** entry field. There is, at this time, no possibility to see data that has already passed.
- **Complete mode.** In this mode data are acquired during a set amount of time. The amount of time is controlled by the entry field **Interval (s)**.

### 3.2.4 Laboratory Guide

An experiment guide was written (Annex IV), in it there is a step by step guide on how to setup the experiment and how to setup the visualization program.

The guide starts off stating the objectives for the experiment. Next it makes a theoretical introduction. Then an explanation of the experimental procedure. After the experiment there is a more detailed explanation on how to achieve the objectives. There

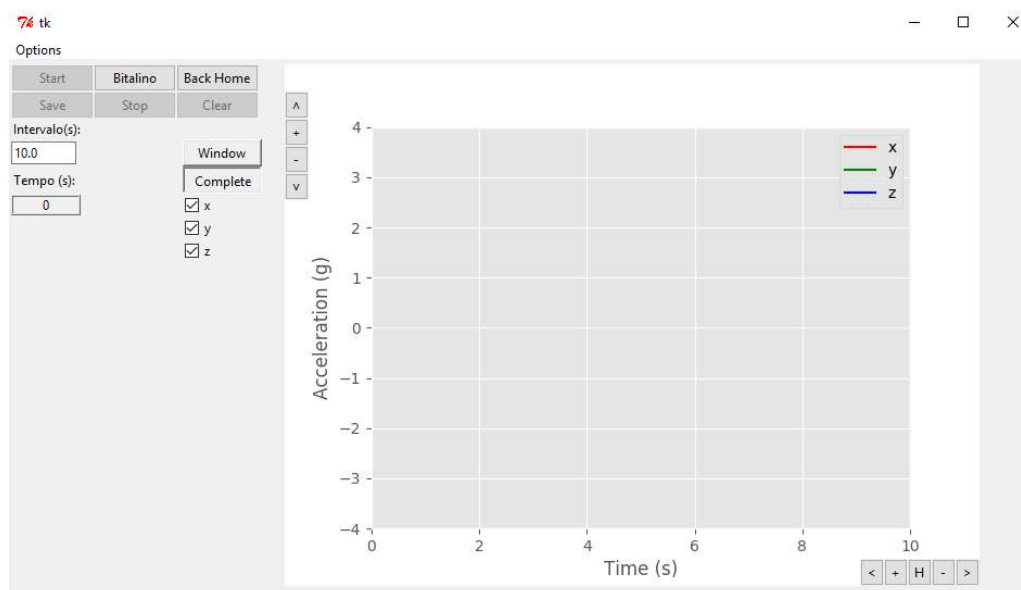


Figure 3.9: The pendulum experiment GUI. For a complete rundown of all the buttons and functionalities see Annex .

is also a section explaining how to use the program, including how to calibrate the accelerometer.

### 3.3 Results and Discussion

#### 3.3.1 Results

The results presented here will follow the necessary steps to complete the experiment and complete the objectives. The resulting acceleration data of a 300 s pendulum motion with our system are plotted in figure 3.10. It is also shown the maxima and minima found by our program. All figures in this section are from the same motion of a 0.600 kg mass suspended on a 0.3 m length string.

The radial acceleration was expected to be 0 at its minima. And in figure 3.10 it is observed this is not the case. Why? Because of the type of accelerometer installed on the BITalino. This accelerometer is a micro electro-mechanical system (MEMS) consisting of a cantilever and a strain sensitive resistor (Fig.3.11). This type of accelerometer relies on measuring the strain on the cantilever. The cantilever has one fixed end, the other end is free and has a mass attached to it. When a force acts on the mass, the cantilever bends and a strain sensitive resistor measures this strain. The strain measurement is proportional to the force acting on the mass.

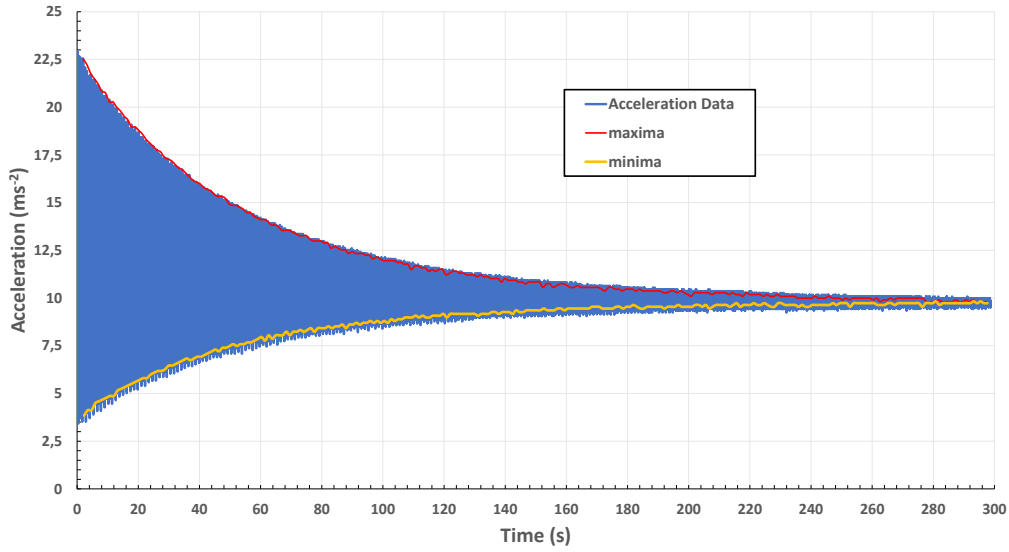


Figure 3.10: The radial acceleration of an oscillating  $0.600 \text{ kg}$  mass with a length of oscillation  $r$  of  $0.3 \text{ m}$ . The starting angle was  $\theta_0 = 65^\circ$ . In red, the local maxima of acceleration and in yellow the local minima.

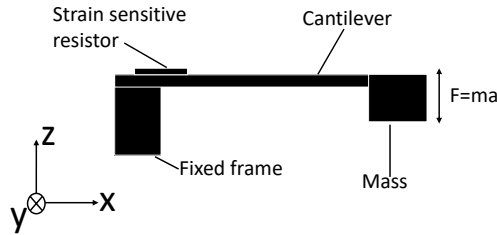


Figure 3.11: MEMS accelerometer diagram.

Our pendulum setup has the BITalino attached to the oscillating mass so that the  $z$  axis accelerometer measures radial acceleration (Fig.3.6). From the point of view of the acceleration due to motion, we could expect the acceleration measured when the pendulum is at rest to be 0. But this is not the case because the cantilever is actually measuring a force. At rest, the  $z$  axis accelerometer measures the gravitational force, as can be seen in figure 3.12.

Still, even with this consideration we expected that the minima should be  $g$ . And, once again, this is not the case. While the tendency of the acceleration is to reach  $g$ , at the beginning of the motion the minima are lower than  $g$ . This too is a consequence of the cantilever accelerometer. When the pendulum hits its maximum amplitude the BITalino itself is inclined, exactly as shown in figure 3.6. Because of this inclination, the gravitational force acting upon the  $z$  axis cantilever is no longer given by  $F_g = mg$ , but rather by  $F_g = mg \cos \theta$ . Therefore, even if the radial acceleration of the pendulum is 0, the measurement is the radial component of the gravitational acceleration given by

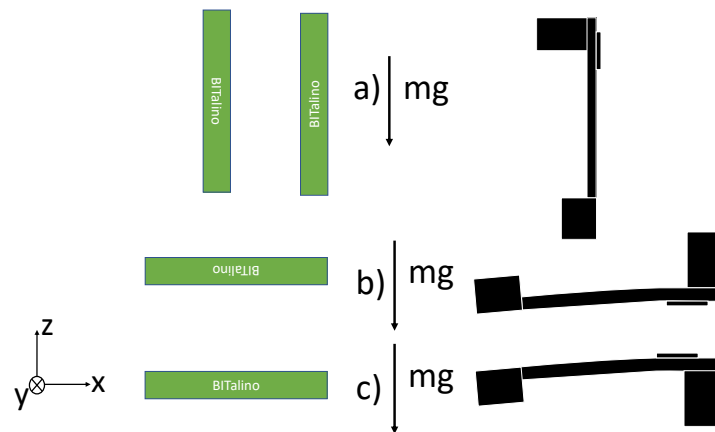


Figure 3.12: z axis accelerometer behavior when the BITalino is stationary in three different positions: a) BITalino is perpendicular to the resting position, in our pendulum system this is equivalent to a  $90^\circ$  angle; b) upside down BITalino; c) the resting position used for our measurements

$a = g \cos \theta$ . This peculiarity turns out to be quite useful as it allows a different measurement of the angle  $\theta_{max}$  given by:

$$a = g \cos \theta_{max} \tag{3.18}$$

$$\theta_{max} = \arccos\left(\frac{a}{g}\right) \tag{3.19}$$

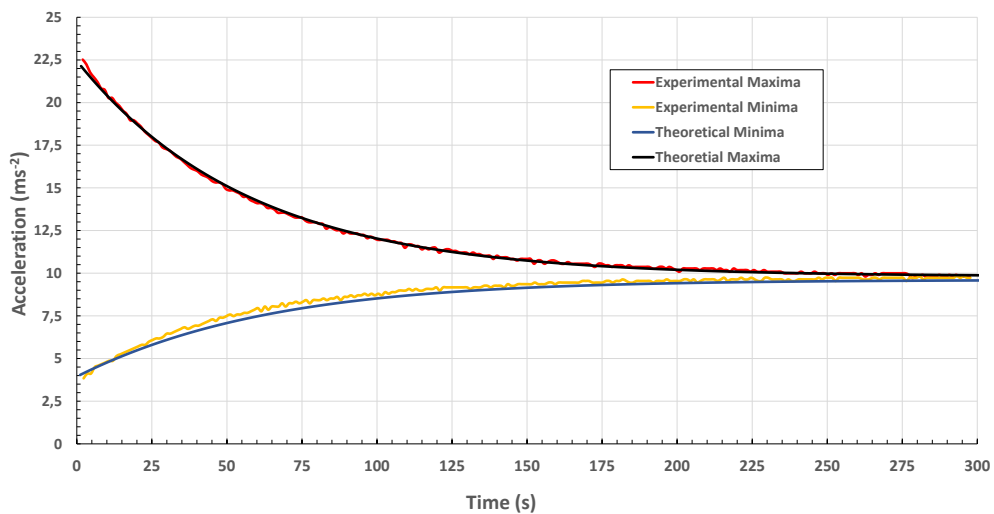


Figure 3.13: This is the type that is expected of the students to find. Two lines with acquired maxima and minima. And two lines where the student must find the  $\tau$  that better fits the experimental data. In this graph  $\tau = 115$  s.

### 3.3.2 Finding $\tau$

The first objective of the pendulum experiment is to find the damping time constant,  $\tau$ , for different masses and different lengths of oscillation. We need to obtain theoretical curves that closely match the experimental maxima and minima. There are two ways to achieve this: a) use equation 3.13, adding the offset  $g = 9.8 \text{ m/s}^2$ , to find theoretical maxima in function of  $\tau$ ; b) or by using equation 3.18. The latter requires an extra step of finding theoretical values for the angle at each minimum time, using expression 3.9. In figure 3.13 it is seen a plot, for  $\tau = 115 \text{ s}$ , with both the experimental and theoretical curves. The optimal  $\tau$  is found by trying different  $\tau$  values until the theoretical curves closely match the experimental. In figure 3.13 we show an example of this, these theoretical curves have  $\tau = 115 \text{ s}$ . Table 3.1 shows typical values of  $\tau$  for different masses and lengths of oscillation.

Table 3.1:  $\tau$  found for pendulum length  $r = 0.32 \text{ m}$ .

Mass (kg)	$\tau$ (s)
0.600	115
0.400	130
0.200	140

If the damping factor is originated from viscous damping, the time constant  $\tau$  should be proportional to the mass of the pendulum. In figure 3.14 it is shown  $\tau$  in function of the oscillating mass. There is no agreement with  $\tau$  being proportional to the mass. So we conclude that viscous damping is not the main damping source for attenuation of the pendulum motion.

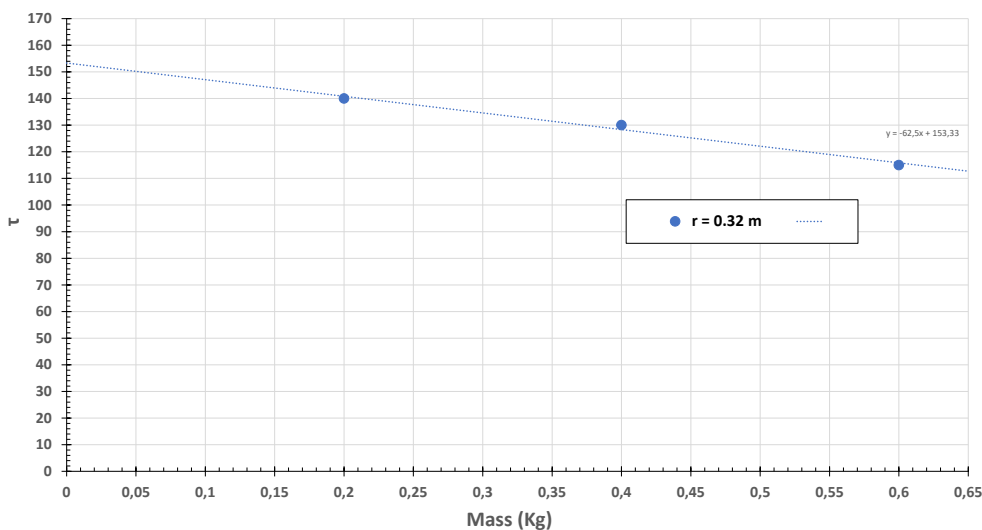


Figure 3.14: Variation of the damping time versus the mass of the pendulum. Note that the proportionality  $\tau \propto m$  expected for viscous damping is not verified.

### 3.3.3 Period of a Real Pendulum

During the entire motion of the pendulum there will be several single oscillations. This can be taken advantage to reach our second objective, which is to verify that the period of one oscillation depends on the angle of oscillation, according to equation 3.16. Because we are interested in the period of only one oscillation, we can assume that there is no damping for the duration of a single oscillation. With this and the acceleration maximum  $a_{max}$  calculated by our program, we can calculate the angle amplitude  $\theta_0$  for each single oscillation with expression 3.20. This expression is derived from equations 3.3 and 3.6:

$$\theta_0^2 = \frac{a_{max}}{r\omega^2} \quad (3.20)$$

As mentioned in the previous section, there is a different way to find  $\theta_0$ . Which uses BITalino's inclination when the mass reaches its maximum amplitude. Figure 3.15 shows a comparison between the angle calculated in both ways, using both maxima and minima of acceleration. In this figure is also plotted the theoretical curve, with  $\tau = 115$  s.

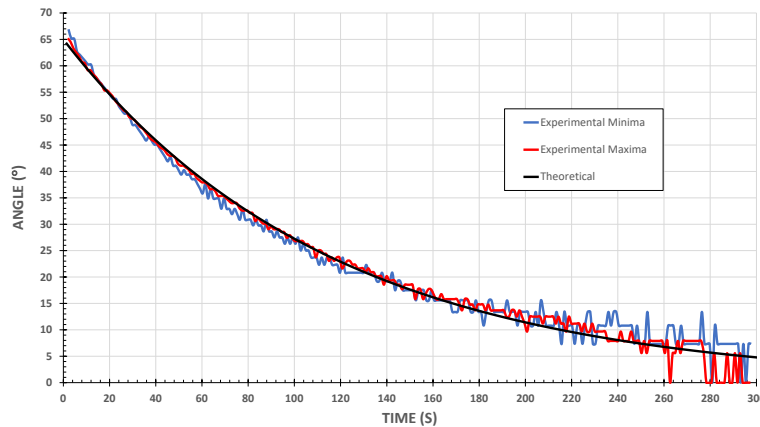


Figure 3.15: Angle of oscillation of a pendulum with  $r = 0.32$  m,  $m = 0.600$  kg. In blues the angle calculated using the minima of acceleration. In red the angles calculated using the maxima of acceleration. In black the theoretical curve.

Results show strong agreement between angle calculated using experimental data, and the expected theoretical results. There is even good agreement between results using the minima and the maxima of acceleration. At the end of the motion it can be seen some discrepancy. At this point of the motion, the oscillation is very subtle. Therefore the variation in acceleration is lower than BITalino's resolution. This in turn makes it impossible for our program to properly detect either maxima or minima.

The period of each oscillation is calculated by our program. Since we save the time at which each maximum occurs the period is just the time between two consecutive maxima. Figure 3.16 shows the calculated period as function of time and the mean period calculated for 5 consecutive oscillations. As predicted by expression 3.16, for large oscillations, the period of oscillation is not constant and increases as the amplitude increases. However, as the motion goes on, i.e. as the amplitude decreases, the period

exhibits a tendency towards a constant. This constant value corresponds to the time period for a small angle oscillation.

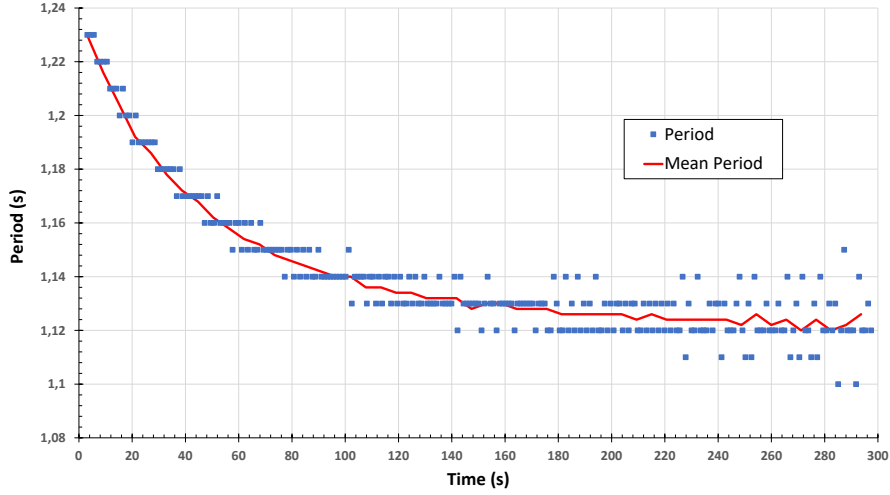


Figure 3.16: Evolution of the period of one oscillation throughout the pendulum motion. In blue dots the period of every oscillation, in red the average for 5 consecutive periods. The period of one oscillation is decreases with amplitude oscillation.

Since variation of both the angle and period of a single oscillation behave as expected throughout the motion there should be a correlation between angle and period of oscillation. In figure 3.17 we plot period of oscillation versus angle amplitude using the data of figures 3.15 and 3.16, the dependence of the period versus the amplitude can be obtained.

To test the correlation, the term  $\varepsilon = \frac{T-T_0}{T_0}$  is introduced. Where  $T$  is the measured period. This term can be related to equation 3.16 by considering  $T_0 = 2\pi\sqrt{\frac{l}{g}}$ , giving:

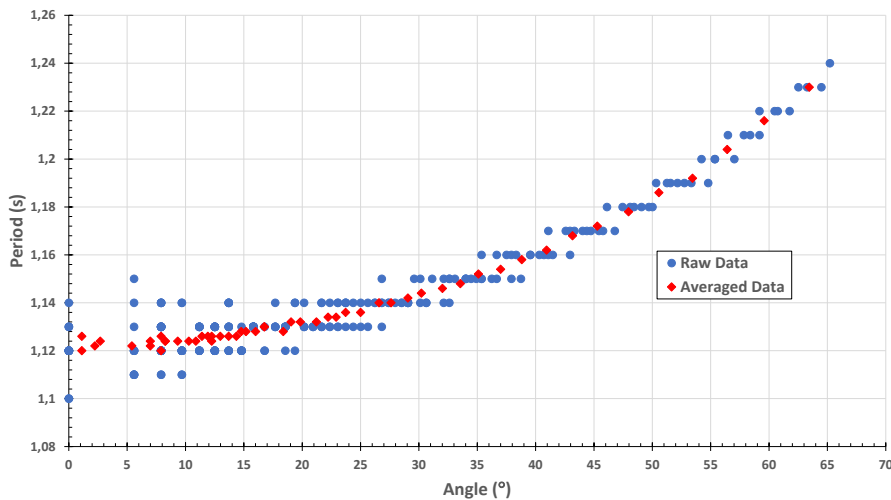


Figure 3.17: Period in seconds versus angle of oscillation in degrees. In blue, the raw data and, in red, the averaged over 5 consecutive points data. Note the non-linear increase of the period for greater angles.

$$T = T_0 \left[ 1 + \frac{1}{16} \theta_0^2 + \frac{1}{3072} \theta_0^4 + \dots \right] \quad (3.21)$$

From this expression we see that  $T$  should be dependent of the squared angle, in radians. If we consider only the first squared term, we get that  $T$  should be linearly dependent of the squared angle:

$$T = T_0 \left[ 1 + \frac{1}{16} \theta_0^2 \right] \quad (3.22)$$

This expression can then related to the term  $\varepsilon$  by:

$$\frac{T - T_0}{T_0} = \frac{1}{16} \theta_0^2 \quad (3.23)$$

Figure 3.18 shows a linear fit of  $\varepsilon$  in function of the squared angle of oscillation. In theory, the slope of this fit should be the coefficient of equation 3.23. The predicted coefficient is 0.0625 and the fit gives 0.0785, which is in the same order of magnitude of the expected value.

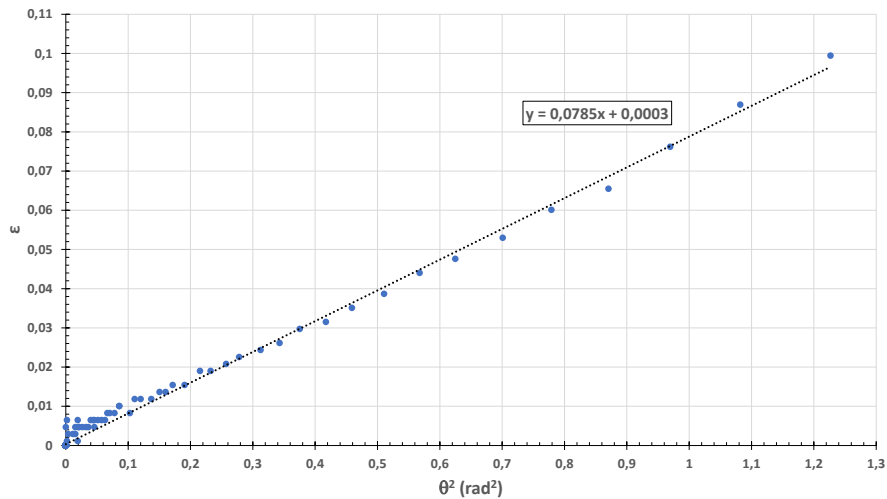


Figure 3.18:  $\varepsilon$  in function of the squared angle. Plot made with the average of 5 consecutive angles and time periods.

In figure 3.19 we plot  $\varepsilon$  versus the squared angle of oscillation for the a pendulum with three different masses. The linear fit for each of these masses gives equations shown in table 3.2. The coefficient found by the linear fit is very similar for each of these oscillation.

Table 3.2: Linear fit equations for masses with pendulum length  $r = 0.32 \text{ m}$ .

Mass ( $kg$ )	Linear Fit
0.200	$\varepsilon = 0.0787\theta^2 + 0.0002$
0.400	$\varepsilon = 0.0798\theta^2 + 0.0004$
0.600	$\varepsilon = 0.0785\theta^2 + 0.0003$



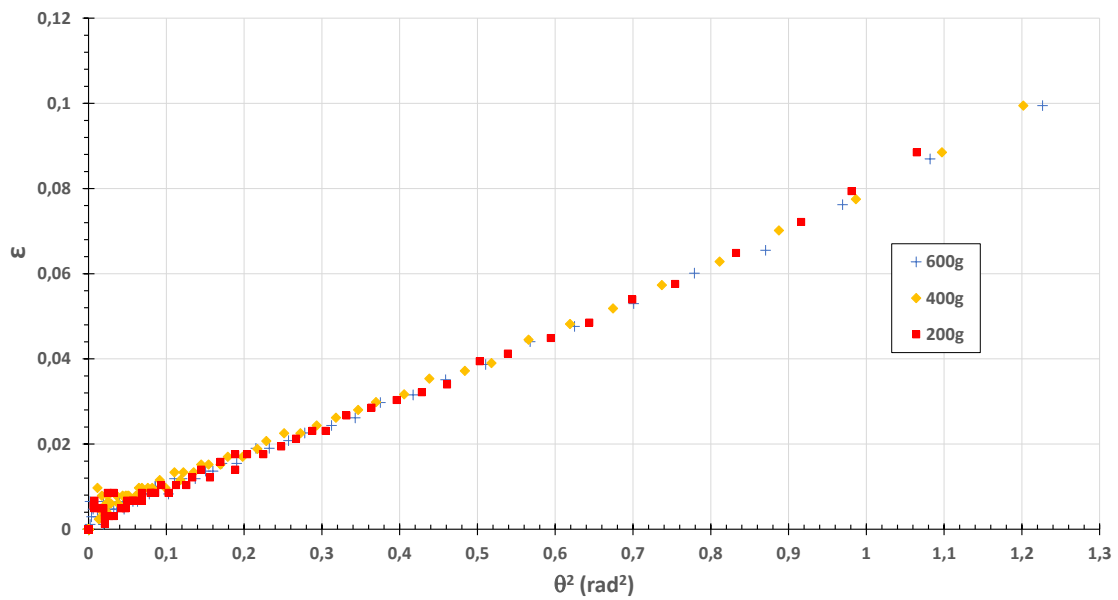


Figure 3.19:  $\varepsilon$  in function of the squared angle. Plot made with the average of 5 consecutive angles and time periods. In blue  $m = 0.600$  kg; in yellow  $m = 0.400$  kg; in red  $m = 0.200$  kg.



## FARADAY INDUCTION: MEASURING MICROVOLTS WITH BITALINO

In this chapter we describe an experiment that verifies Faraday's induction law. This is done by measuring the tension induced on a coil moving through a stationary magnetic field. The tension is measured in function of magnetic field intensity, area, and velocity.

We aim to make improvements in measurement visualization and cost. Currently, at the FCT-UNL physics laboratory, this experiment uses a very flexible voltmeter, it has many possible ranges of measurement, from  $[-100, 100] \mu V$  to  $[-3, 3] V$ . However, the visual reading is made with a pointer, this may lead to inaccurate measurements. Our goal is to facilitate more precise measurements of tension, and, at the same time, to provide the data recorded in a file in order to have a more reliable treatment.

In section 4.1 a theoretical contextualization is presented. Section 4.2 shows the setup for this experiment. And results of this experiment using the BITalino are presented in section 4.3.

### 4.1 Theoretical Formulations

Faraday's law of induction says that when the magnetic flux  $\Phi$  through a surface  $A$ , whose boundary is a wire loop, changes, the wire loop acquires an electromotive force  $\varepsilon$ , which is given by the rate of change of the magnetic flux over time:

$$\varepsilon = -\frac{d\Phi}{dt} \quad (4.1)$$

The change in flux can be caused either by changing the intensity of magnetic field  $B$ , or by changing the surface area  $A$ :

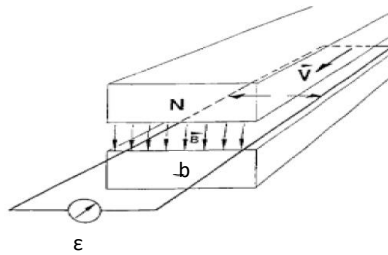


Figure 4.1: Conductive ring in a static magnetic field

$$\Phi = \int \vec{B} \cdot d\vec{A} \quad (4.2)$$

In this experiment the wire loop is moved out of a uniform magnetic field at constant velocity  $v$ . The surface area inside the field varies, therefore so does the magnetic flux. An electromotive force  $\varepsilon$ , proportional to the flux variation is, in this way, created on the wire loop. The loop used in this experiment has a rectangular form of width  $b$ , see figure 4.1. Thus the flux variation with time is given by:

$$\frac{d\Phi}{dt} = B \frac{dA}{dt} \quad (4.3)$$

And so, combining expressions 4.2 and 4.3 we get:

$$\varepsilon = Bbv \quad (4.4)$$

this expression indicates proportionality between the electromotive force created in the loop,  $\varepsilon$  and three variables. To verify proportionality with magnetic field intensity  $B$ , the intensity of the magnetic field can be changed by changing the number of magnets. Proportionality between  $\varepsilon$  and velocity  $v$  can be tested by moving the loop at different speeds. Lastly, the relation between area  $A$  and  $\varepsilon$  can be verified by changing the width  $b$  of the loop.

## 4.2 Experimental Setup

### 4.2.1 System Summary

Figure 4.2 shows a diagram of this experiment setup. Induction system (1) is the structure in the wire loop moves through the magnetic field. The magnetic field is created by magnets laid out in pairs. The wire loop is mounted on a cart pulled by rotor (2) at a constant speed controlled by a power source. There are 3 different sized loops, which can be individually connected to microvoltmeter (3).

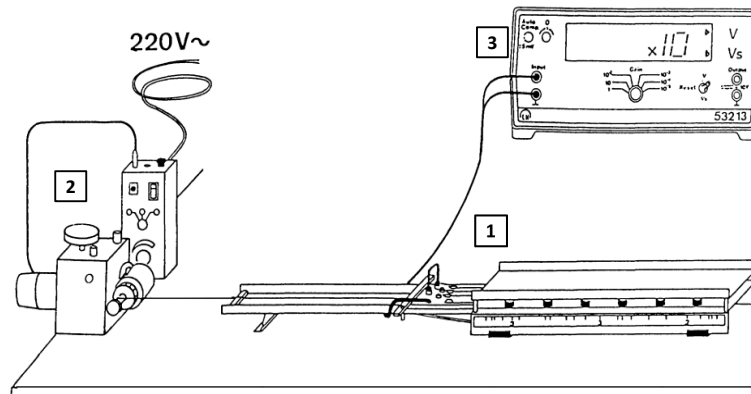


Figure 4.2: Diagram of the experimental system. (1) is the induction system. (2) is an electric rotor. (3) is a voltmeter.

In this experiment the induced tension can vary from  $20 \mu V$  to  $300 \mu V$ . BITalino has a resolution of 10 bit with an input range of up to  $3.3 V$ . This means that BITalino's smallest measurement is of around  $3 mV$ . Then, it is not possible to directly use BITalino to measure the tension induced on the wire loop. For this reason, it is necessary to build an electronic circuit that amplifies the induced voltage.

In Figure 4.3 we see the assembled experimental setup for this experiment. There are a few additions to what is shown in Figure 4.2: a switch to turn the rotor on and off, and the BITalino connected to the pre-amplifier which is connected to the wire loop. BITalino sends the voltage data to a computer connected via Bluetooth. In this setup, the desk microvoltmeter is still used to verify that the data measured with BITalino are identical to what is read by the microvoltmeter. In the final experimental setup for the lab the desk microvoltmeter will not be used.

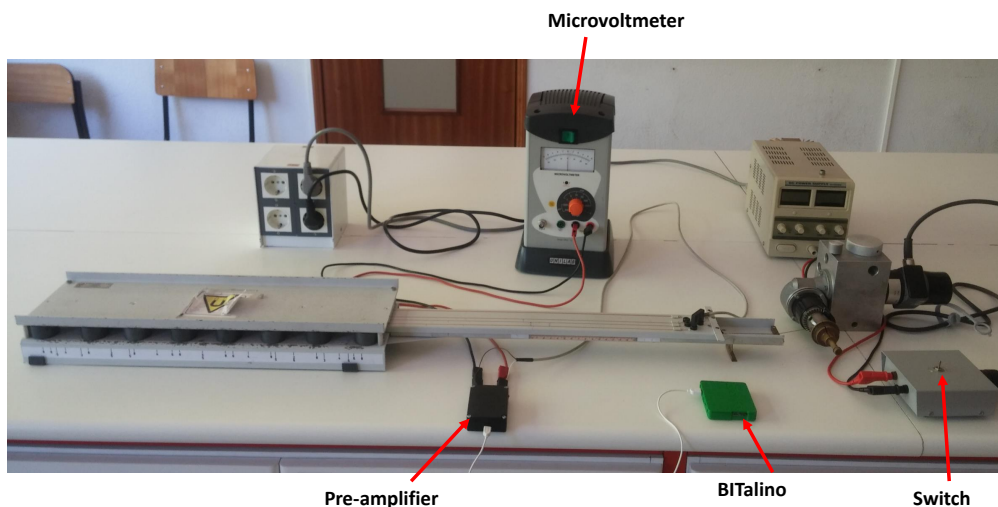


Figure 4.3: Faraday induction experimental setup.

### 4.2.2 Circuit Dimensioning

As was mentioned, it was necessary to build an electronic circuit. The final circuit is shown in Figure 4.4.

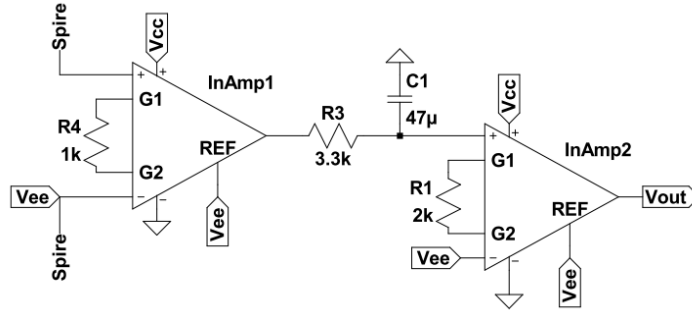


Figure 4.4: A two stage amplifier, for a total of 5151 gain, with a low-pass 1 Hz filter to reduce noise.

The circuit uses two INA 333 instrumentation amplifiers. These amplifiers are specialized for low power functionality, featuring low power single-supply and rail-to-rail output [16]. This means they are perfect to use with the BITalino.

The BITalino can supply either 3.3 V or 1.65 V of output power. Having the intermediate point 1.65 V gives some flexibility in designing the circuit. Our goal with this circuit is to measure a range of  $[-300; +300] \mu V$  with BITalino.

The circuit is a two stage pre-amplifier. On the first stage, the difference between the two extremities of the loop is amplified by a gain of 101.  $V_{ee} = 1.65 V$  are supplied to this amplifier's reference pin, and to the loop. The latter is needed because the inputs of the INA 333 instrumentation amplifier must be approximately 0.1 V above the negative supply voltage. The former makes it so the output of the first stage is referenced to  $V_{ee}$ . This way if the inducted tension is  $V_{inducted}$ , then output of the first stage will be given by:

$$V_{out\ InAmp1} = V_{ee} + V_{inducted} * 101 \quad (4.5)$$

Because BITalino's analog input port can only read positive voltage, the output of this second stage cannot be negative. However, the configuration of the first stage solves this problem. As negative induced voltages will be referenced to  $V_{ee}$ , meaning they will be positive values.

The second stage then, only needs to further amplify the signal to fully utilize BITalino's measurement range. For this, the negative input voltage is set to  $V_{ee} = 1.65 V$  and the positive input is the output of the first stage. The reference pin is once again set to  $V_{ee} = 1.65 V$ . This second stage is set to a gain of 51, making a total gain of 5151 for the

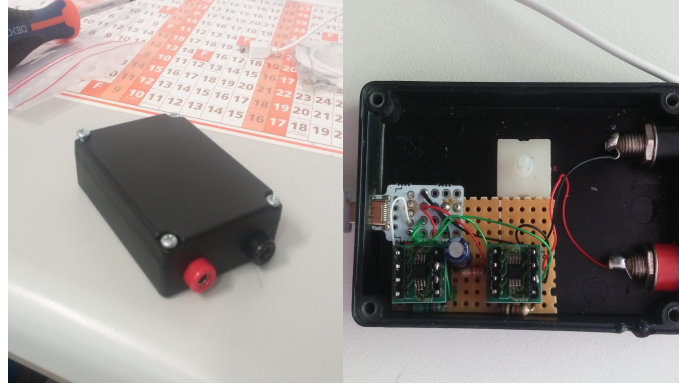


Figure 4.5: The pre-amplifier assembled on a box. Banana connectors to connect to the wire loops and a USB connector to connect the amplifier to BITalino.

whole circuit. Now, considering the output of this circuit as  $V_{out}$ , the voltage induced on the loop is given, in  $\mu V$ , by:

$$V_{inducted}(\mu V) = \frac{V_{out} - 1.65}{51 * 101} \quad (4.6)$$

The circuit also has a low-pass filter of 1 Hz to reduce noise. Equation 4.7 give the low-pass filter cutoff frequency,  $f_c$ .

$$f_c = \frac{1}{2\pi RC} \quad (4.7)$$

In this circuit, the filter was set to  $R = 3.3 \text{ k}\Omega$  and  $C = 47 \text{ }\mu F$ . Which gives a cutoff frequency of 1 Hz. In section 4.2.3 some tests to optimize the filter are presented.

Figure 4.5 shows the built pre-amplifier assembled on a box with the necessary connectors.

### 4.2.3 Filter Optimization: Cutoff Frequency Effect

Reducing noise is the filter objective, but using a filter implies adding a response time to the circuit. In order to minimize this delay and maximize noise reduction a few different filter configurations were tested. It was decided to fix the capacitance at  $47 \text{ }\mu F$ , and test different resistance values. Table 4.1 shows the tested resistances and the respective cutoff frequencies. The resistances were limited to easily available resistances.

Table 4.1: Cutoff frequency for different resistances.

Resistance ( $k\Omega$ )	$f_c$ (Hz)
1.5	2.26
3.3	1.03
4.5	0.77

From Figure 4.6 it is concluded that the best configuration for this application is a filter with a cutoff frequency of 1 Hz. With a load resistance of  $1.5 \text{ k}\Omega$ , the filter has

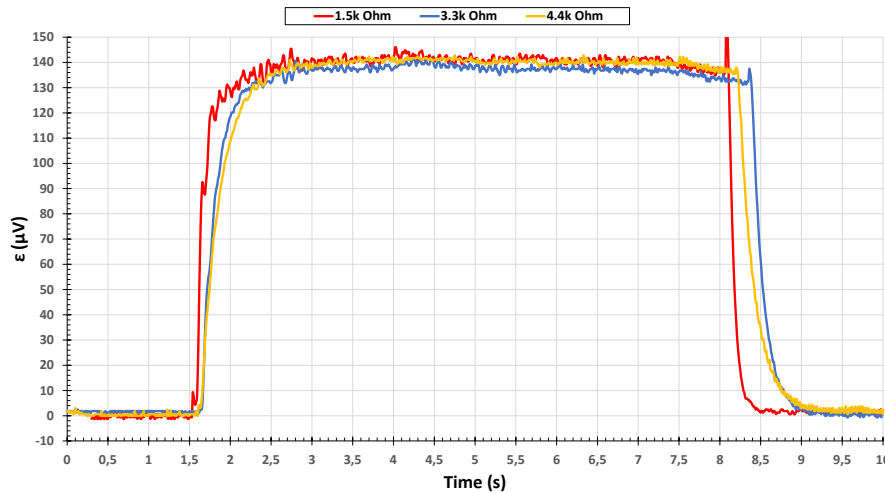


Figure 4.6: Cutoff frequency response to different load resistances. Higher resistance means the filter takes longer to act.

faster response time, meaning there is a lesser amount of data lost. However, as expected, because of the higher cutoff frequency it has worse noise filtering performance. With a load resistance of  $4.5\text{ k}\Omega$ , the filter has good noise filtering performance. But has a slower response time when compared to the filter with a load resistance of  $3.3\text{ k}\Omega$ . For these reasons, it was decided to build the pre-amplifier with a low-pass filter with cutoff frequency,  $f_c$ , of  $1.03\text{ Hz}$ .

#### 4.2.4 Python Program

A transfer function is applied to the sampled values. This function must take into consideration the pre-amplifier, equation 4.6 and the conversion from bit to volt of the digital signal:

$$V_{out}(V) = \frac{ADC * 3.3}{1024} \quad (4.8)$$

ADC is the sampled value in bit.  $V_{out}$  can then be inserted in equation 4.6 to get the tension inducted on the loop.

With this transfer function, and knowing BITalino's input analog port used has 10 bit resolution, it is found this homemade microvoltmeter has a resolution of  $1\ \mu V$ .

The resulting data acquired during an experiment of Faraday induction are shown in figure 4.7, this is data exported to an Excel worksheet.

It is possible to see that when the loop is not moving, the tension measured is not zero (Fig. 4.7). This small offset appears because the INA 333 instrumentation amplifier cannot have an output of exactly  $0\text{ V}$ . Therefore, at the output of the first amplification stage there is a residual voltage that gets amplified on the second stage. Resulting in the offset observed in figure 4.7.



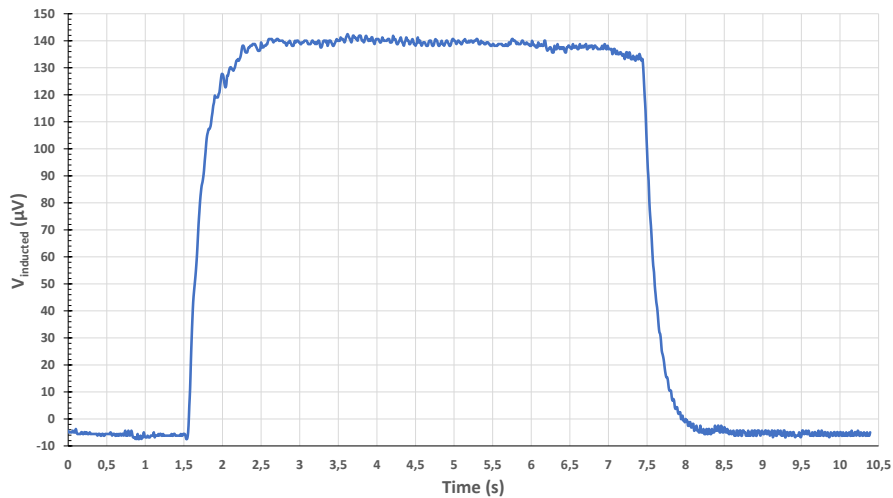


Figure 4.7: Typical plot of induced tension in function of time.

The graphical interface for this experiment (Fig. 4.8) is very similar to the Pendulum experiment. The only difference is the addition of a window which shows the last read value.

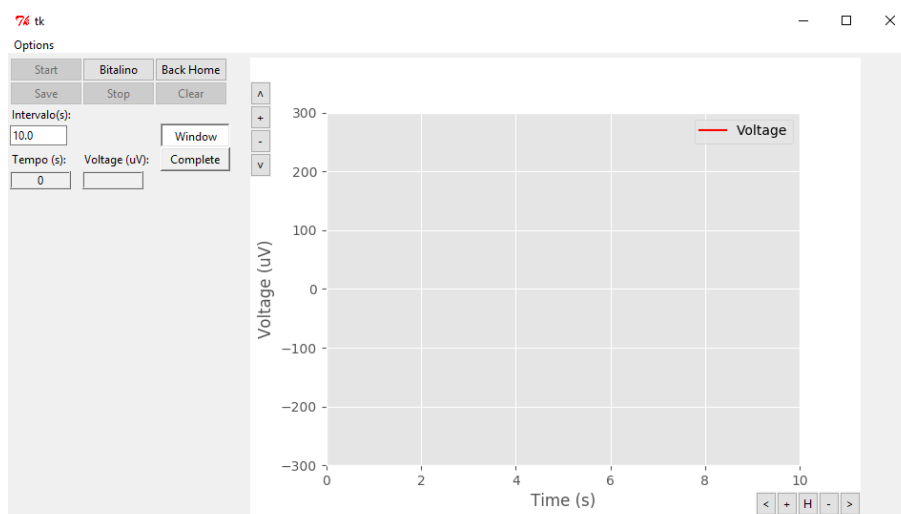


Figure 4.8: The Faraday induction experiment GUI.

### 4.3 Results and Discussion

The objective of this experiment is to determine the linear dependence of the electromotive force  $\varepsilon$  induced on a loop with: surface area, magnetic field intensity, and velocity.

The results were treated using an Excel worksheet. Sources of error include: non-homogeneous magnetic field due to misalignment of the magnets; noise introduced by the pre-amplifier; velocity not constant throughout the movement.

Figure 4.9 shows electromotive force  $\varepsilon$  as a function of time, for loop widths of  $0.020\text{ m}$ ,  $0.028\text{ m}$ , and  $0.040\text{ m}$ .

Figure 4.10 plots  $\varepsilon$  as a function of time, for velocities of  $v = 0.020\text{ m/s}$ ,  $v = 0.040\text{ m/s}$ , and  $v = 0.080\text{ m/s}$ .

Figure 4.11 plots  $\varepsilon$  as a function of time, for different number of magnets.

The induced electromotive force  $\varepsilon$ , shown in the tables and figures below, is the average of the points over the duration of the movement.

Table 4.2: Results obtained for  $v = 0.067\text{ m/s}$  and 8 pairs of magnets, with varying loop width.

$b\text{ (m)}$	$\varepsilon\text{ (}\mu\text{V)}$	$B\text{ (T)}$
0.020	65	$5.02 \cdot 10^{-2}$
0.028	94	$5.02 \cdot 10^{-2}$
0.040	135	$4.90 \cdot 10^{-2}$

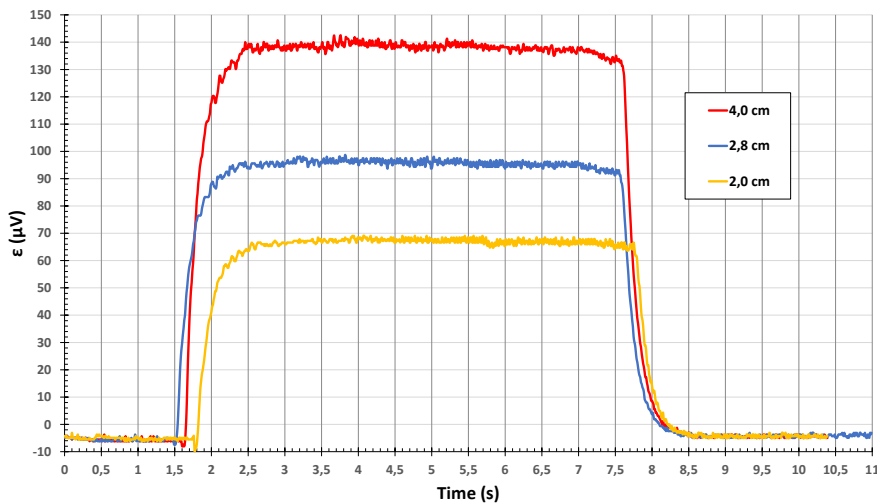


Figure 4.9: Voltage induced, at constant speed and constant magnetic field intensity, on a loop of varying widths: in red, a width of  $0.040\text{ m}$ ; in blue width of  $0.028\text{ m}$ ; and in yellow width of  $0.02.0\text{ m}$ . As predicted the voltage at width  $0.040\text{ m}$  is double the voltage induced on a loop of  $0.02.0\text{ m}$  width.

Table 4.3: Results obtained for 8 pairs of magnets and  $b = 0.04\text{ m}$ , with varying velocity.

$v\text{ (m/s)}$	$\varepsilon\text{ (}\mu\text{V)}$	$B\text{ (T)}$
0.018	35	$4.92 \cdot 10^{-2}$
0.035	70	$5.03 \cdot 10^{-2}$
0.068	137	$5.05 \cdot 10^{-2}$

All results agree with the theoretical formulations. From figures 4.12, 4.13 and 4.14 we verify that there is indeed linear dependence between the electromotive force induced and the variables studied.

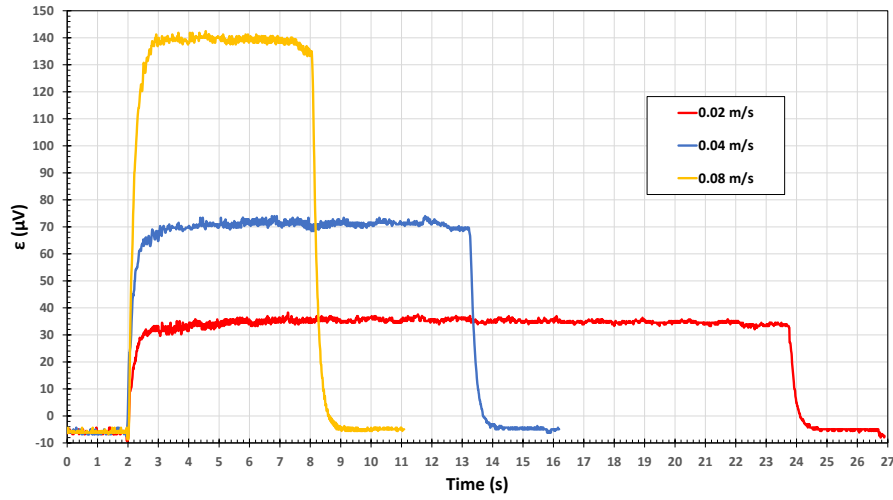


Figure 4.10: Voltage induced on a loop of constant width, moving through a static magnetic field at different velocities: in red,  $v = 0.020 \text{ m/s}^{-2}$ ; in blue  $v = 0.040 \text{ m/s}^{-2}$ ; and in yellow  $v = 0.080 \text{ m/s}^{-2}$ .

Table 4.4: Results obtained for  $v = 0.086 \text{ m/s}$  and  $b = 0.04 \text{ m}$ , with varying magnetic field intensity.

Nº Magnets	$\epsilon$ ( $\mu V$ )	$B$ (T)
2	30	$1.15 \cdot 10^{-2}$
4	62	$2.39 \cdot 10^{-2}$
5	81	$3.10 \cdot 10^{-2}$
6	94	$3.61 \cdot 10^{-2}$
8	133	$5.13 \cdot 10^{-2}$

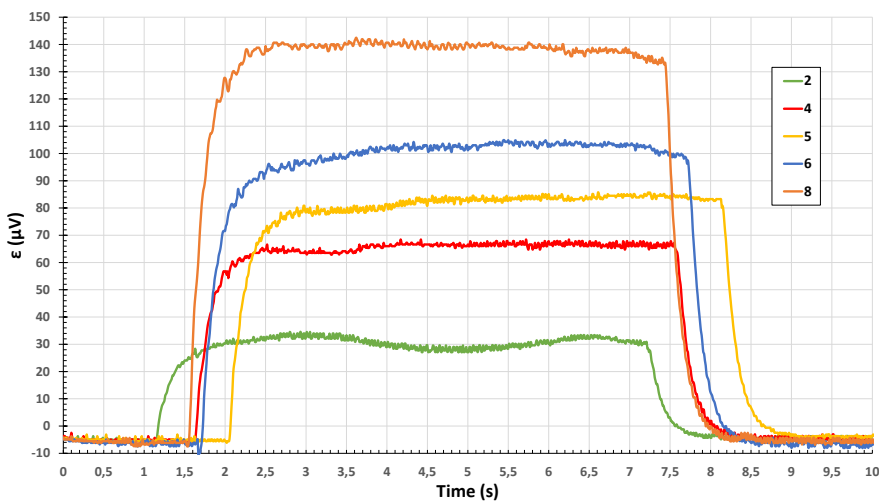


Figure 4.11: Voltage induced on a loop of constant width, moving, at constant velocity, through a static magnetic field, with varying intensities.

The average calculated magnetic field intensity of 8 magnets was  $4.99 \cdot 10^{-2} T$ . The manufacturer guarantees, for 8 pairs of magnets, a magnetic field of  $5 \cdot 10^{-2} T$ , which gives a 0.2% error.

Most importantly, we show that the BITalino can be used as a replacement for the expensive desk microvoltmeter. Even more so, it can be done cheaply. The pre-amplifier we built cost under €10, the only material we had to buy was PCB, two INA 333 instrumentation amplifiers, and a case for our circuit. The rest were off the shelf components, i.e. resistances, capacitors, connectors, etc. With just a BITalino we cannot measure microvolts, but it is possible to build a simple circuit that circumvents this limitation.

Our program proved to be reliable in visualizing and saving data. Having real time data visualization, with possibility to actually see how the experiment is progressing, allows for quick readjustments to the experimental setup. In this case it proved most useful for checking if the magnets were properly aligned. There is also the fact that, since data are readily available for treatment on an Excel worksheet, it is possible to quickly check the validity of the acquired data.

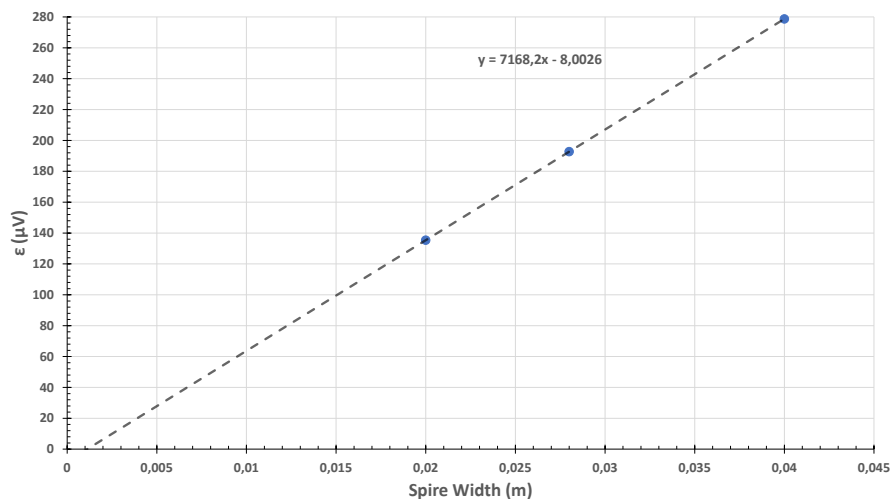


Figure 4.12: Plot of averaged  $\varepsilon$  in function of  $b$ . With a linear fit equation.

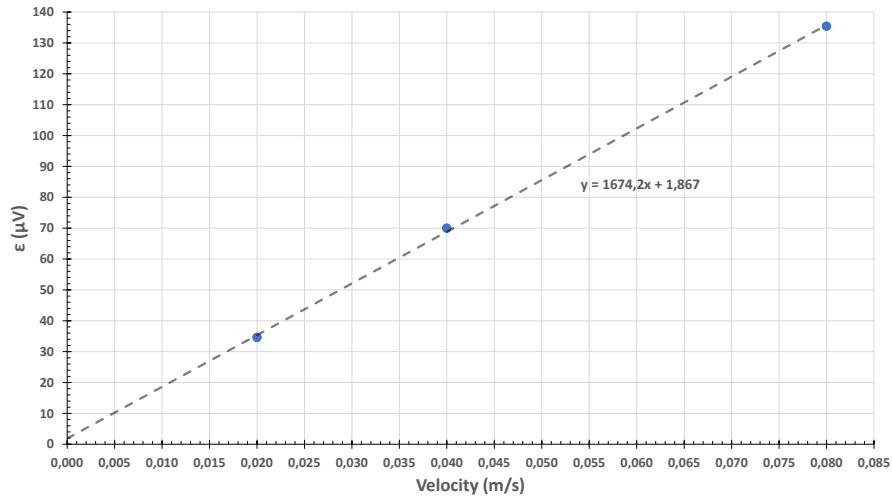


Figure 4.13: Plot of averaged  $\varepsilon$  in function of  $v$ . With a linear fit equation.

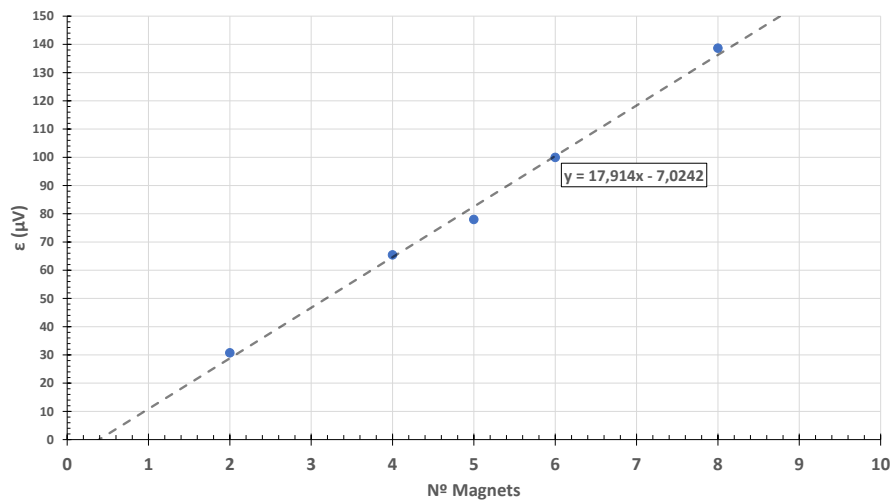


Figure 4.14: Plot of averaged  $\varepsilon$  in function of number of magnets. With a linear fit equation.



## MEASURING TEMPERATURE WITH BITALINO

In previous sections, it was shown how BITalino could be utilized in experiments for Mechanics (Cf. Chapter 3) and Electromagnetism (Cf. chapter 4). In this chapter, we build a cheap digital thermometer to use in Thermodynamics experiments. The thermometer is a resistance temperature detector Pt100 (platinum resistor, 100  $\Omega$  at 0  $^{\circ}\text{C}$ ) whose resistance variance will be measured using a Wheatstone bridge.

In section 5.1 the experimental setup is described. Results and discussion are presented in section 5.2

### 5.1 Experimental Setup

#### 5.1.1 Circuit Dimensioning

The digital thermometer is built around a resistance temperature detector, RTD. As the name indicates, RTD is a type of sensor in which a temperature change corresponds to a resistance change. The Pt100 is one of the most commonly used RTD, they are rather cheap and often used as pedagogical sensors.

The Pt100 is made of Platinum and has a nominal resistance of 100  $\Omega$  at 0  $^{\circ}\text{C}$ . In these type of sensors the relationship between resistance and temperature is defined as the amount of resistance change per degree of temperature change. This temperature coefficient, usually denoted by  $\alpha$ , in its linear approximation between 0  $^{\circ}\text{C}$  and 100  $^{\circ}\text{C}$ , is given by equation 5.1:

$$\alpha = \frac{R_{100} - R_0}{100^{\circ}\text{C} \cdot R_0} \quad (5.1)$$

where,  $R_{100}$  and  $R_0$  are the resistance of the material at 100  $^{\circ}\text{C}$  and 0  $^{\circ}\text{C}$ , respectively.  $\alpha$  is usually presented in  $\Omega/(\Omega \cdot ^{\circ}\text{C})$ . Usually for the Pt100  $\alpha = 0.00385 \Omega/(\Omega \cdot ^{\circ}\text{C})$ .

From equation 5.1 it is then possible to derive an expression that says what is the resistance,  $R_x$ , of the Pt100 at temperature  $T$ :

$$R_x = R_0(1 + \alpha * T) \quad (5.2)$$

For larger temperature ranges, there are tables and more precise expression available better than expression 5.2.

The circuit that correlates a change in resistance to a change in voltage the well known Wheatstone bridge (Fig. 5.1). In this bridge, only resistance  $R_x$  varies, the other resistances are used to adjust parameters in the bridge. Resistances  $R_1$  and  $R_2$  control the bridge current and the output range of the bridge. Resistance  $R_3$  is the reference resistance that controls the resistance value  $R_x$  necessary for the bridge to be in equilibrium. Therefore, we have the known leg  $R_2/R_3$ , and the unknown leg  $R_1/R_x$ . If the ratio between the two resistances in the known leg is equal to the ratio between the resistances in the unknown leg, the bridge is said to be balanced. When the bridge is in balance voltage  $V_G$  is zero. A change in  $R_x$  will cause the ratio in the unknown leg to be different, unbalancing the bridge. This results in  $V_G$  being different from zero.

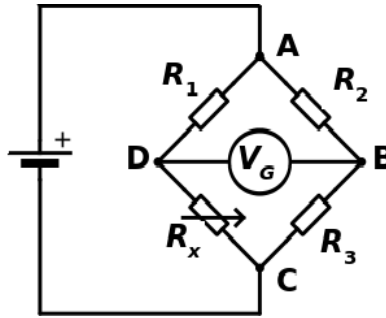


Figure 5.1: Wheatstone bridge.  $R_x$  is where the Pt100 is connected.  $R_3$  is the reference resistance.

The unbalance voltage  $V_G$  is given by equation 5.3 where  $V_S$  is the supply voltage of the power source (in this case the power source is BITalino). If  $R_1 = R_2$ , the bridge will be balanced if  $R_x = R_3$ . The reference resistance sets the point at which the bridge is balanced. If  $R_x < R_3$  then the unbalance voltage will be negative:

$$V_G = \left( \frac{R_x}{R_1 + R_x} - \frac{R_3}{R_3 + R_2} \right) \cdot V_S \quad (5.3)$$

since BITalino measures  $V_G$ , the only unknown variable in this circuit is  $R_x$ , our Pt100 resistance. Expression 5.3 can be used to determine the resistance of the Pt100.

A limitation of the Wheatstone bridge is that it does not have completely linear behavior. This non-linearity can be attenuated by using larger resistances  $R_1$  and  $R_2$ . However, by increasing these resistances, the current flowing through resistance  $R_x$  and  $R_3$  decreases, leading to lower bridge sensitivity. A compromise has to be made. We choose



$R_1 = R_2 = 600 \Omega$  for these reasons, these resistance values also guarantee that the current flowing through the Pt100 is not over  $10 \text{ mA}$ .

The power supply for this circuit is the BITalino itself, which implies maximum supply voltage  $V_S = 3.3 \text{ V}$ . The unbalance voltage  $V_G$ , for the two reference resistances discussed in section 5.2, will be in the range  $[0; 400] \text{ mV}$  (Table 5.1). Therefore, we amplify this signal using an operational amplifier. The necessary gain is dependent on the range of temperatures being measured. Figure 5.2 shows the schematic for a circuit with a gain of 10 using an operational amplifier.

Table 5.1: Theoretical bridge voltage for the two reference resistances used in section 5.2.

	$R_x (\Omega)$	Temperature	$V_G (\text{mV})$
$R_{ref} = 93.2 \Omega$	96	$-10 \text{ }^\circ\text{C}$	12
	100	$0 \text{ }^\circ\text{C}$	27
	119	$50 \text{ }^\circ\text{C}$	102
	139	$100 \text{ }^\circ\text{C}$	172
$R_{ref} = 22.1 \Omega$	24	$75 \text{ K}$	8
	53	$150 \text{ K}$	146
	81	$225 \text{ K}$	273
	110	$300 \text{ K}$	389

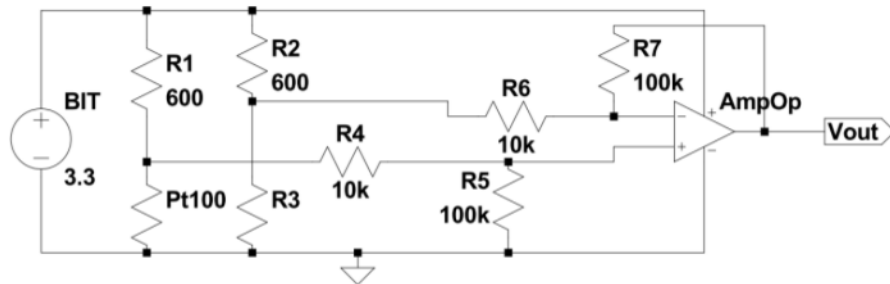


Figure 5.2: Circuit schematic for temperature measurement with a Pt100 and a BITalino.

The goal is to measure two temperature ranges. For general use in a thermodynamics experiments, i.e. verifying water's triple point, a temperature range of  $[263; 383] \text{ K}$  is established. And, to verify the Leidenfrost effect, the range  $[70; 300] \text{ K}$  is chosen. The resolution of this thermometer will depend on BITalino's 10 bit resolution and on the range of temperature to be measured. In Table 5.2 we see the theoretical ranges of measurement, for an ideal circuit, and the respective resolution.

Table 5.2: Measurement ranges and respective resolutions.

$\Delta T (\text{K})$	$\Delta R (\Omega)$	<i>bits</i>	Resolution
120	46.2	10	$0.1 \text{ K/bit}$
240	92.4	10	$0.2 \text{ K/bit}$

The circuit was assembled on a breadboard using off the shelf components. The amplifier used was a LM 358 operational amplifier. Which does not have rail-to-rail capacity, but still allows single supply operation. As can be seen in its datasheet, [17], the LM 358 has output voltage range much lower than the positive supply voltage. So, instead of having voltage range of  $[0; 3.3]$  V, the practical range using this amplifier is  $[0; 1.9]$  V. In figure 5.3 it is seen the saturation of the LM 358 at around 1.9 V. The theoretical curve in this plot is obtained by multiplying the theoretical bridge output of different  $R_x$  values (Eq. 5.3) by the gain ( $gain = 10$ ). The experimental curve is obtained from measurements, with a voltmeter, of the circuit output, with  $gain = 10$ .

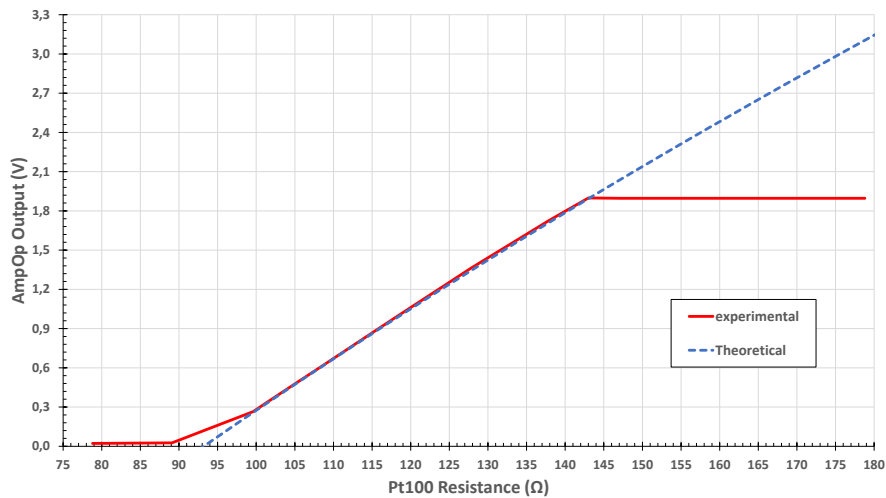


Figure 5.3: The effect of saturation of the LM 358 in red, as measured with a reference resistance  $R_2 = 93.2 \Omega$  and a gain of 10. In blue the output of an ideal operational amplifier, for a circuit with the same reference resistance and gain.

Because of the saturation of the LM 358, the gain must be set in such a way that the maximum temperature to be measured corresponds to 1.9 V at the output of the amplifier. The found values for the two ranges mentioned are, respectively:  $gain = 10$  and  $gain = 5$ . This has a significant impact on the resolution of the thermometer, which can be seen by comparing the resolution in tables 5.2 and 5.3. We observe that using this operational amplifier results in a a loss of resolution by a factor of two.

Table 5.3: Practical measurement ranges and respective resolutions.

$\Delta T$ (K)	$\Delta R$ ( $\Omega$ )	bits	Resolution
120	46.2	10	0.2 K/bit
240	92.4	10	0.4 K/bit

### 5.1.2 Python Program: GUI

The function that converts the digital signal sampled in bit to a temperature value is divided in three parts. The first transforms the sampled value ADC to the voltage of the

Wheatstone bridge,  $V_G$ :

$$V_G(V) = \frac{ADC * 3.3}{1024} * \frac{1}{gain} \quad (5.4)$$

from equation 5.3, the equation to determine the resistance of the Pt100 is derived:

$$R_x (\Omega) = R_1 \cdot \frac{\left(\frac{V_G}{V_S} + \frac{R_3}{R_2+R_3}\right)}{1 - \frac{V_G}{V_S} - \frac{R_3}{R_2+R_3}} \quad (5.5)$$

Finally, having obtained resistance  $R_x$  it is now possible to substitute this value in equation 5.2 to obtain the temperature of the Pt100.

The interface for this experiment is shown in figure 5.4.

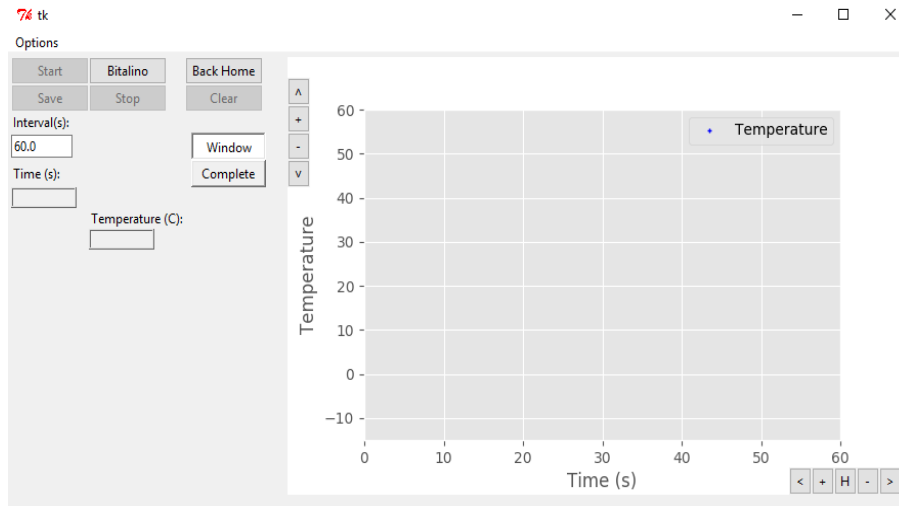


Figure 5.4: The thermometer GUI.

## 5.2 Results and Discussion

Possible sources of error include: parasitic resistance in the Pt100 wire; and parasitic voltage in the circuit. The parasitic resistance comes from the wire connecting the Pt100 to the circuit and can be estimated to be  $0.03 \Omega$ . In all cases, this parasitic resistance can be neglected as it is much lower BITalino's own resolution. A  $0.03 \Omega$  resistance variance corresponds to a change in temperature of  $0.08 K$ , which is negligible considering the resolution of the BITalino and the temperature ranges being measured.

### 5.2.1 Thermometer for [263;383] K range

To properly assess the reliability of the circuit, the Pt100 was replaced by different resistances. Each resistance is measured before being assembled on the circuit. In figure 5.5 is seen a plot of temperature measured with BITalino in function of the resistance, in blue, and a plot of the expected temperature versus resistance, in red. The circuit for

these data was dimensioned for temperature measurement within the range [263;383] K, which means the reference resistance is  $R_3 = 93.2 \Omega$  and the gain is  $gain = 10$ .

Figure 5.6 shows error  $\Delta T$ : the difference between the temperature calculated,  $T_m$ , with resistance  $R_x$  measured with BITalino, and the temperature calculated with the resistance manually measured by an ohmmeter,  $T_e$ :

$$\Delta T = T_m - T_e \quad (5.6)$$

In the same figure we show the actual gain of the circuit, in black. This gain is found experimentally by calculating  $gain = V_{out}/V_G$ , where  $V_G$  is the unbalanced voltage of the bridge, manually measured by a voltmeter, and  $V_{out}$  is the output voltage of the circuit, measured with BITalino.

It can be concluded that temperature measurements are mostly within the expected values. The resolution of this thermometer is 0.2 K (table 5.3) and, from figure 5.6, it is possible to see that  $\Delta T$  is mostly within the resolution values. It is also possible to notice that, as the temperature approaches the upper limit of set range, readings become inaccurate. This is also reflected on the effective gain of the circuit, as  $V_G$  increases in accordance with the resistance increase, the output voltage of the amplifier stays the same. Which translates into lower and lower gain.

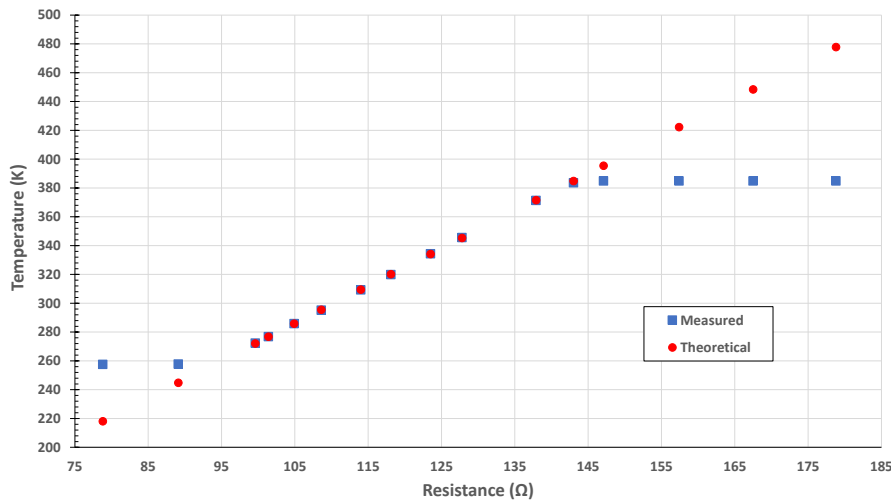


Figure 5.5: Measured and theoretical temperatures in function of test resistances.

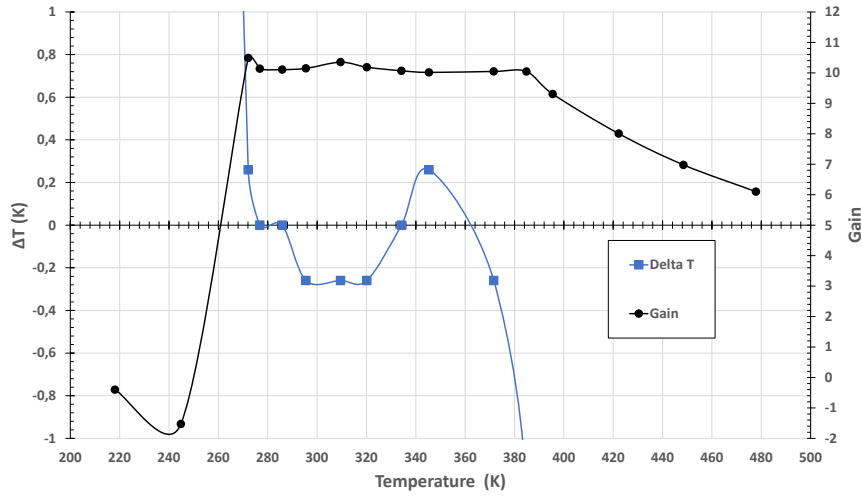


Figure 5.6: In blue the difference between measured and expected temperature,  $\Delta T = T_m - T_e$ , in function of the Temperature. In black the gain of the circuit.

### 5.2.2 Thermometer for [70;300] K range

In figure 5.7 we plot, in the blue line, temperature measured with BITalino versus resistance and, in the red line, temperature expected versus resistance. The circuit was dimensioned for a temperature measurement range of [70;300] K, which means the reference resistance is  $R_3 = 22.1 \Omega$  and the gain is  $gain = 5$ . Similarly to the analysis of the previous section, figure 5.8 shows the error,  $\Delta T = T_m - T_e$ , of temperature calculated,  $T_m$ , compared to expected temperature,  $T_e$ , in blue. The actual gain of the circuit is shown in black.

It can be concluded that temperature measurements are not within the expected values. In figure 5.8 we can see a relevant difference between expected values and measured values. Given that the resolution of this thermometer is 0.4 K (Table 5.3), this error is always higher than the resolution, which could indicate an issue in the circuit. The error is consistently around  $\Delta T = 0.5 K$ , this could indicate an offset somewhere in the circuit. The fact that the gain is consistently around its expected value of 5 shows the amplifier behaves appropriately, in which case the error must originate somewhere else.

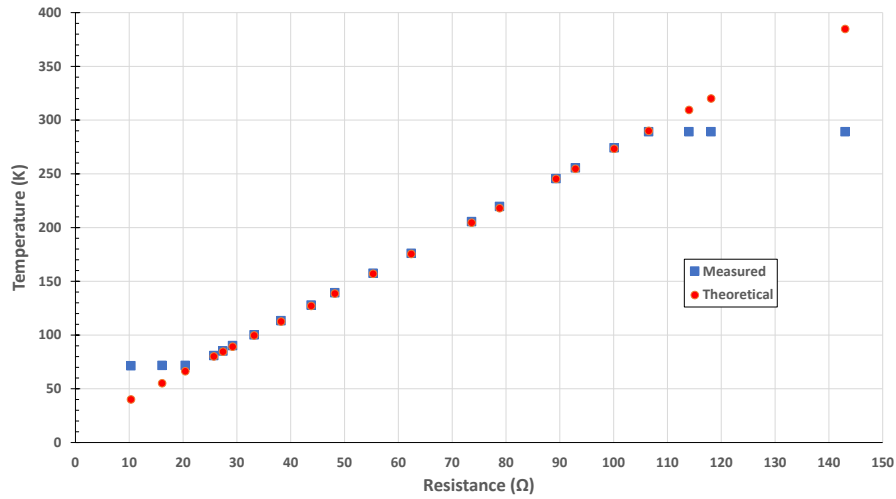


Figure 5.7: Measured and theoretical temperatures in function of test resistances.

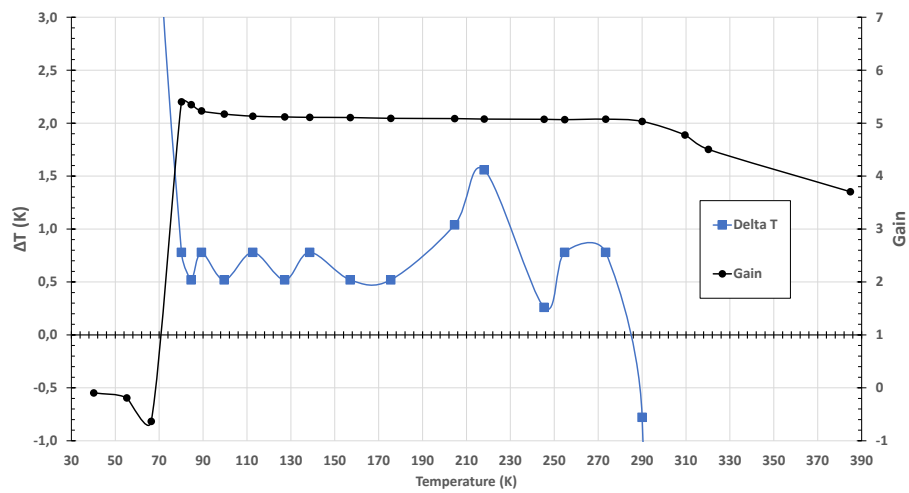


Figure 5.8: In blue the difference between measured and expected temperature,  $\Delta T = T_m - T_e$ , in function of the Temperature. In black the gain of the circuit.

## CONCLUSION

### 6.1 Final Remarks

The main goal of this work was to apply new technologies to didactic physics experiments. To help in this development, a BITalino - a miniaturized, wireless acquisition system developed by PLUX - was employed.

This thesis marks the start of this project, with the following goals: to develop a new pendulum experiment to be used in the Mechanics Physics Laboratory; to show how the BITalino can be complemented with homemade sensors - such as a microvoltmeter or a thermometer - that allow the BITalino to be used as an acquisition system in different experiments, of varying disciplines. For the latter, it was elected to choose one experiment from the disciplines of Electromagnetism and Thermodynamics. Together all three experiments really show how versatile a miniaturized acquisition system with wireless communication can be.

The pendulum experiment, here devised, was a success. The experiment we design gives new possibilities to study the pendulum and its movement. The pendulum is a truly rich experiment, and with the experiment described in this thesis, it is possible to provide to the students an experiment that showcases some more advanced phenomena. For instance, it was possible with this experiment to determine the damping time constant of a real pendulum, as well as, to find the dependence of the period with the amplitude, phenomenon usually not very easy to measure. An experiment guide to help the students was written. An obstacle has, however, been encountered. The data acquired in this experiment are not of simple analysis, it goes beyond a regular pendulum experiment, in which, usually, only the period is measured. In this experiment we are forced to think with acceleration in mind, and this is not very common or even intuitive. It might be more challenging, but for that same reason it can also be a bigger motivator for the student to

understand the physics behind it.

The second objective was achieved in two parts. First, as a representative of the Electromagnetism discipline, the Induction Faraday experiment was chosen. The results obtained were, for the most part, well within the expected. The offset mentioned in section 4.2, does not affect the results of the calculations. It can, however, induce some misunderstanding on the student performing the experiment. There are two possible ways to handle this situation: implement a calibration function, which sets the zero of the read data, to correspond to the sampled value when the inducted voltage is null; manually subtract on the Excel worksheet; or just to leave it as it is, since there is no impact on the results. Both ways have pros and cons, for now it was elected to go with the latter rather than the former. This way there is no 'hidden' data manipulation nor any 'mysterious' calibration. It is a *plug and play* experiment.

Finally, for Thermodynamics, a digital thermometer using the BITalino was built. PLUX provides two temperature sensors in their store [18]. However, one is expensive and the other has a fixed temperature range. As we have mentioned before, the purpose is to have cheaper experiments, and more flexibility. Here there were some results better than others. At the range of an experiment to determine the triple point of water, for instance, very good results were obtained. The temperature readings were accurate within the resolution of the BITalino itself. However, moving to a larger temperature range of [65;300] K, temperature readings show a systematic error of around 0.5 K which, at this moment, is not clear why it shows up.

In conclusion, all goals were achieved. Some secondary objectives were also set and achieved. Chief among them, to make a visualization program that is easy to use and shows the acquired data in real time. In the Faraday induction experiment this is quite relevant: as a matter of fact, the signal to be measured appears during a time relatively short, difficulting its reading. To have data stored in a file allows a much more reliable and objective treatment. Temperature readings with this program are also made more interesting by showing the data in a plot of temperature throughout time, which allows for immediate comparisons with earlier measurements.

## 6.2 Future Work

So far it has been proven that BITalino is a valuable tool for a didactic physics laboratory. However, some improvements can still be made to the digital thermometer. It is clear that the obtained resolution is quite low, there are a few causes here. Chief among them is the fact that a proper amplifier was not used. The LM 358 operational amplifier, while reliable and accessible, is not ideal for this sort of application. Here, a low power rail-to-rail instrumentation amplifier is a must that allows for full access to BITalino's range. Moreover, in order to change temperature range of the circuit used in section 5.2, it is necessary to change a few components. With the operational amplifier used, in order to change the range of measurement of the thermometer we must change the reference



resistance and the gain resistance of the amplifier; the gain resistances to be changed are, at least, two, and as many as four; this can be a tedious and laborious task, especially on a soldered circuit. However, there is no escaping the 10 bit limitation imposed by BITalino. If possible, this could be a good help in improving resolution of future sensors. Finally, it would be good to assemble the thermometer circuit in a PCB board with a switch that would allow for different temperature ranges.

Having established that the BITalino is a reliable substitute for commercially available acquisition systems, it now becomes important to build a repertoire of experiments that use the BITalino. Specifically in Mechanics experiments, some work could be done to find new ways to utilize the BITalino, i.e. to study collisions, or angular motion. Of course, this repertoire would also include guides on how to assemble different complementary accessories, of which the microvoltmeter and digital thermometer would be a part.

One last improvement worth mentioning would be to make a proper GUI. Time, and knowledge, were big constraints in this work. While Python is a remarkably powerful language, there are better solutions to make user interfaces. However, at the start of this project this was not known. As such, a project to make a proper, robust, reliable program would be an excellent addition to this work.



## BIBLIOGRAPHY

- [1] S. Gerstner and F. X. Bogner. “Cognitive Achievement and Motivation in Hands-on and Teacher-Centred Science Classes: Does an additional hands-on consolidation phase (concept mapping) optimise cognitive learning at work stations?” In: *International Journal of Science Education* 32.7 (2010), pp. 849–870.
- [2] C. E. Hmelo-Silver. “Problem-Based Learning : What and How Do Students Learn ?” In: *Educational Psychology Review* 16.3 (2004), pp. 235–266.
- [3] N. G. Holmes, C. E. Wieman, and D. A. Bonn. “Teaching critical thinking.” In: *Proc Natl Acad Sci U S A* 112.36 (2015), pp. 11199–11204.
- [4] C. Wieman and N.G. Holmes. “Measuring the Impact of Introductory Physics Labs on Learning.” In: *Journal of Computer Assisted Learning* 10.4 (1994), pp. 251–260.
- [5] M. C. Rytting. “Comparison of Simulation and Hands-On Labs in Helping High School Students Learn Physics Concepts.” Doctoral dissertation. Brigham Young, 2016, p. 182.
- [6] H. P. Da Silva, A. Lourenço, A. Fred, and R. Martins. “BIT: Biosignal Igniter Toolkit.” In: *Computer Methods and Programs in Biomedicine* 115.1 (2014), pp. 20–32.
- [7] D. Meyer. *This \$35 Computer Just Passed a Major Sales Milestone*. 2016. URL: <http://fortune.com/2016/09/08/raspberry-pi-10-million/> (visited on 08/13/2017).
- [8] *Fritzing Creator Kit*. Fritzing. 2017. URL: <http://fritzing.org/fritzing-creatorkit/> (visited on 09/23/2017).
- [9] *SparkFun Inventor’s Kit v3.3*. SparkFun. 2017. URL: <https://www.sparkfun.com/products/13969> (visited on 09/23/2017).
- [10] H. P. Da Silva, A. Fred, and R. Martins. “Biosignals for everyone.” In: *IEEE Pervasive Computing* 13.4 (2014), pp. 64–71.
- [11] *BITalino Is A Low Cost, Modular Bio-Signal Sensor Kit That Makes It Quicker and Easier To Build Medical Devices and Health Tracker Apps*. TechCrunch. Sept. 5, 2017. URL: <https://techcrunch.com/2013/09/05/bitalino/> (visited on 09/23/2017).
- [12] *BITalino - Biomedical Equipment | Low-cost Toolkit*. PLUX. 2017. URL: <https://bitalino.com> (visited on 09/23/2017).

## BIBLIOGRAPHY

---

- [13] *Final Version of DataStudio*. PASCO Scientific. 2017. URL: <https://www.pasco.com/datastudio/> (visited on 09/23/2017).
- [14] *Motion Sensor PS-2103A Instruction sheet*. 012-09625B. Retrieved: 13-09-2017. PASCO. URL: [https://www.pasco.com/file\\_downloads/Downloads\\_Manuals/PASPORT-Motion-Sensor-Manual-PS-2103A.pdf](https://www.pasco.com/file_downloads/Downloads_Manuals/PASPORT-Motion-Sensor-Manual-PS-2103A.pdf).
- [15] *PASCO 850 Universal Interface Model No. UI-5000*. 012-12355B. Retrieved: 13-09-2017. PASCO. URL: [https://www.pasco.com/file\\_downloads/Downloads\\_Manuals/850-Universal-Interface-Manual-UI-5000.pdf](https://www.pasco.com/file_downloads/Downloads_Manuals/850-Universal-Interface-Manual-UI-5000.pdf).
- [16] *INA333 Micro-Power (50  $\mu$ A), Zero-Drift, Rail-to-Rail Out Instrumentation Amplifier*. SBOS445C. REVISED DECEMBER 2015. Texas Instruments. July 2008. URL: <http://www.ti.com/lit/ds/symlink/ina333.pdf>.
- [17] *LMx58-N Low-Power, Dual-Operational Amplifiers*. SNOSBT3I. REVISED DECEMBER 2014. Texas Instruments. Jan. 2000. URL: <http://www.ti.com/lit/ds/symlink/lm158-n.pdf>.
- [18] *Sensors - PLUX Store*. PLUX. 2017. URL: [store.plux.info/15-BITalino-sensors](http://store.plux.info/15-BITalino-sensors) (visited on 09/23/2017).



## ANNEX 1 BITALINO PLUGGED DATASHEET

# BITalino (r)evolution Freestyle Kit Data Sheet

BFK 160616

## SPECIFICATIONS

- > **Sampling Rate:** 1, 10, 100 or 1000Hz
- > **Analog Ports:** 4 in (10-bit) + 2 in (6-bit)  
+ 1 auxiliary in (battery) + 1 out (8-bit)
- > **Digital Ports:** 2 in (1-bit) + 2 out (1-bit)
- > **Communication:** Bluetooth or BLE
- > **Range:** up to ~10m (in line of sight)
- > **Sensors:** EMG; ECG; EDA; EEG;  
ACC; LUX; BTN
- > **Actuators:** LED; BUZ
- > **Size:** 100x65x6mm
- > **Battery:** 500mA 3.7V LiPo (rechargeable)
- > **Consumption:** ~65mA
- > **Accessories:** 3x Electrode cable with  
30cm; 2x Electrode cable with 10cm;  
5x Crimp pins; 2x Molex Sherlock plug  
(3-pin); 4x Molex Sherlock (4-pin) socket;  
5x Electrodes; 1x ProtoBIT

## FEATURES

- > Ideal for hardware prototyping
- > Stackable to enable compact form factors
- > Raw data acquisition
- > Battery charger
- > Easy-to-use
- > Affordable

## APPLICATIONS

- > Psychophysiology
- > Biomedical projects
- > Electrical engineering
- > Human-Computer Interaction
- > Robotics & Cybernetics
- > Physiology studies
- > Biofeedback

## GENERAL DESCRIPTION

Our unique BITalino (r)evolution Freestyle kit has all blocks as individual components, making it ideal for wearables. Kits include the basic parts to get started. Our cross-platform OpenSignals software enables instant data visualization and recording, while the APIs provide low-level access from third party and custom applications.

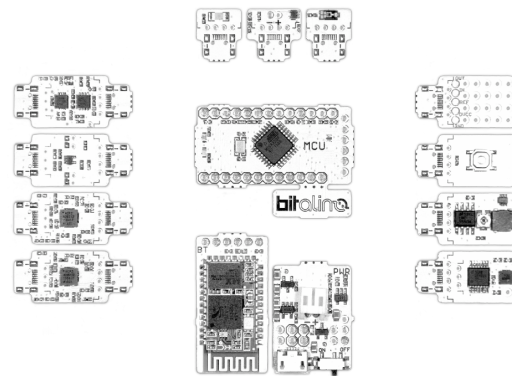


Fig. 1. Blocks are provided as individual components, so you can let your imagination run free and create bespoke devices; available with Bluetooth (Fig. 4) or BLE (Fig. 5).

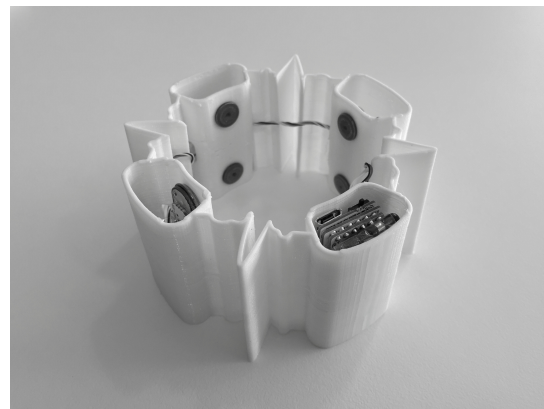


Fig. 2. BITalino Freestyle kits enable you to easily create wearables and miniaturized biosignal acquisition devices (some components in the image are optional accessories).

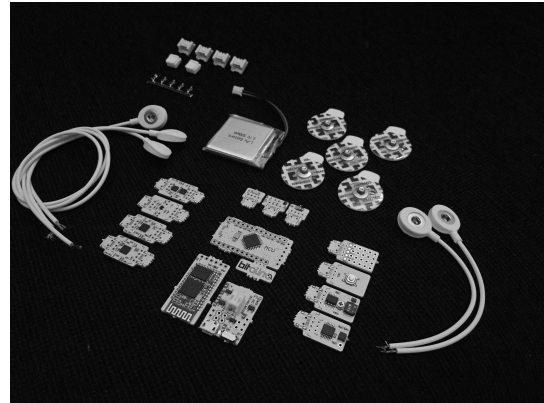


Fig. 3. Parts and accessories included in the kit.

# bitalino

PLUX – Wireless Biosignals, S.A.  
Av. 5 de Outubro, n. 70 – 8.  
1050-059 Lisbon, Portugal  
bitalino@plux.info  
<http://bitalino.com/>

REV A

© 2016 PLUX 

This information is provided "as is," and we make no express or implied warranties whatsoever with respect to functionality, operability, use, fitness for a particular purpose, or infringement of rights. We expressly disclaim any liability whatsoever for any direct, indirect, consequential, incidental or special damages, including, without limitation, lost revenues, lost profits, losses resulting from business interruption or loss of data, regardless of the form of action or legal theory under which the liability may be asserted, even if advised of the possibility of such damages.



BEWARE: DIRECT OR INDIRECT COUPLING TO THE MAINS MAY RESULT IN SHOCKING HAZARD



# BITalino (r)evolution Freestyle Kit Data Sheet

## FUNCTIONAL BLOCKS

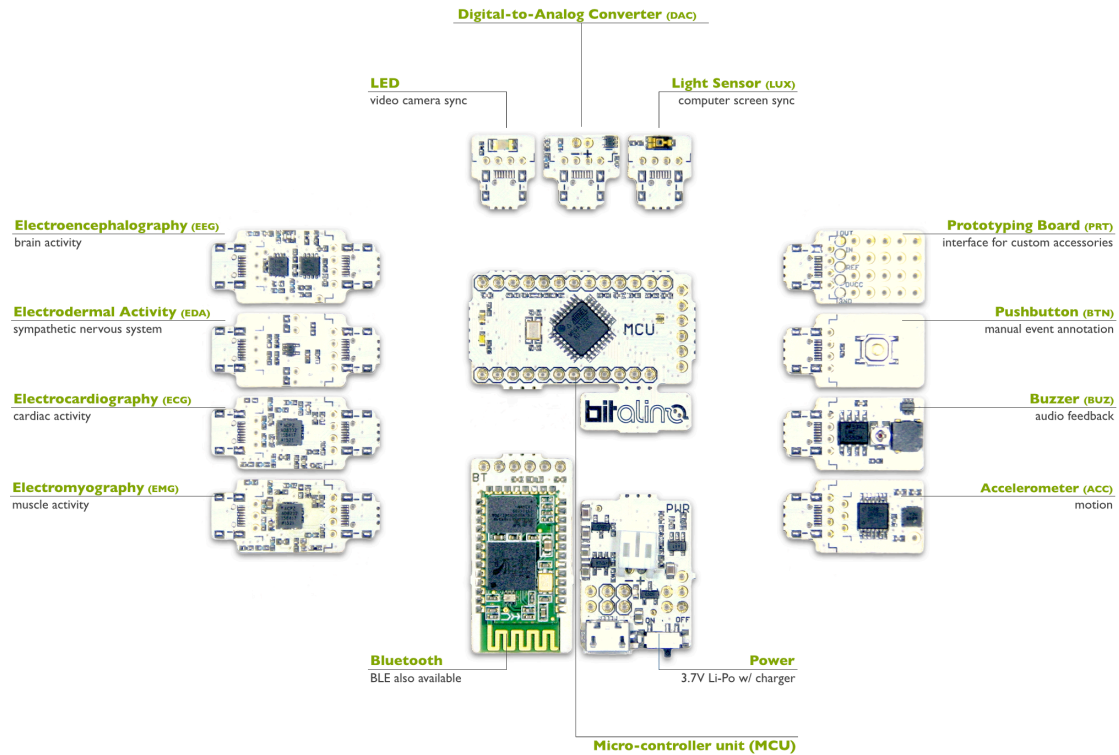


Fig. 4. BITalino (r)evolution Freestyle with Bluetooth connectivity.

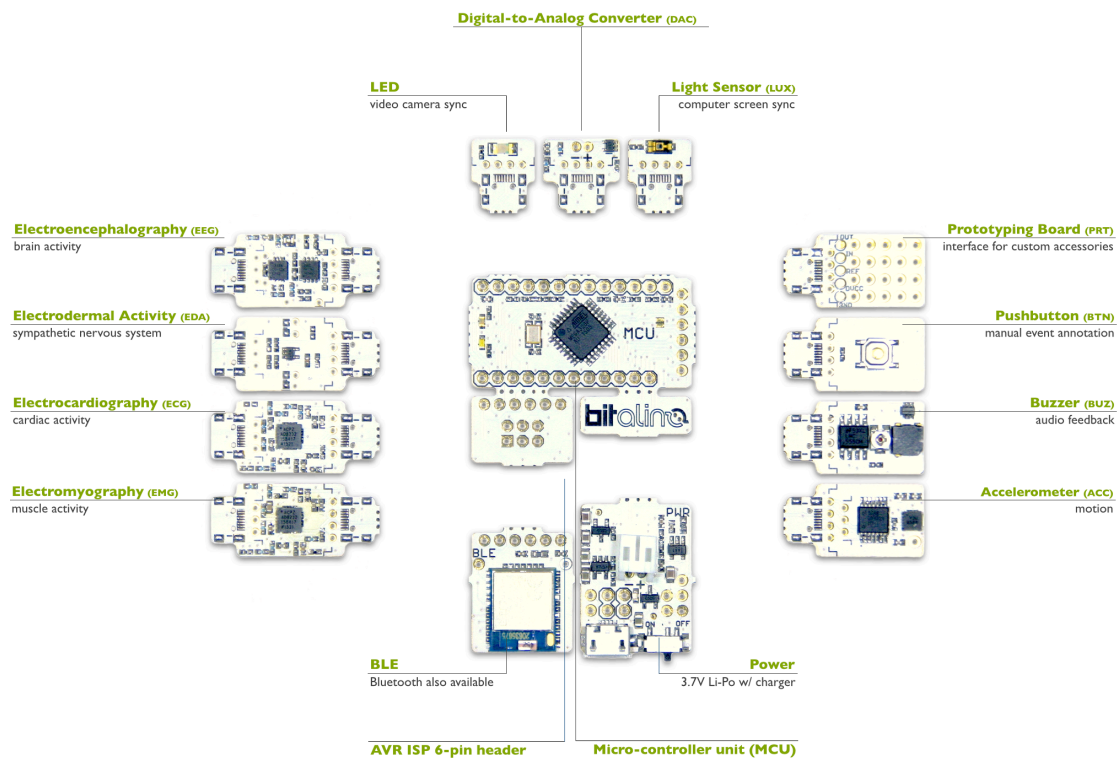


Fig. 5. BITalino (r)evolution Freestyle with BLE connectivity.





A  
N  
N  
E  
X



## ANNEX 2 ACCELEROMETER DATASHEET

# Accelerometer (ACC) Sensor Data Sheet

---

## **TRANSFER FUNCTION**

[-3g, 3g]

$$ACC(g) = \frac{ADC - C_{min}}{C_{max} - C_{min}} \cdot 2 - 1$$

$ACC(g)$  – ACC value in g-force ( $g$ )

$ADC$  – Value sampled from the channel

$C_{min}$  – Minimum calibration value<sup>1</sup>

$C_{max}$  – Maximum calibration value<sup>1</sup>

## **ORDERING GUIDE**

<b>Part #</b>	<b>Description</b>
SENS-ACC-NC	Accelerometer (ACC) without connectors
SENS-ACC-UCE6	Accelerometer (ACC) with UC-E6 socket for seamless plug & play connection to a BITalino (r)evolution Plugged or Core
SENS-ACC-SHER4	Accelerometer (ACC) with a Molex Sherlock 4-pin socket for easy power and signal cable connection or pin breakout using PCB wires

---

<sup>1</sup> Calibration values are determined by performing a very slow 360° rotation of the sensor board to force the accelerometer to cross the gravity-imposed  $-1g$  and  $1g$  in each axis. It is recommended that filtering or averaging of the data is performed to remove natural tremors (e.g. shaky hands) as illustrated in Fig. 2.



## ANNEX 3 HOW TO CALIBRATE BITALINO'S ACCELEROMETER

The calibration of the accelerometer isn't a mechanical one. Rather it's about finding the sampled values in bits to which known acceleration points correspond. These acceleration values are  $\pm g$ . So by performing a full rotation over any axis the accelerometer is 'forced' to read both  $+g$  and  $-g$ . Which should be the variables  $C_{max}$  and  $C_{min}$ , respectively, in equation III.1.

$$ACC(g) = \frac{ADC - C_{min}}{C_{max} - C_{min}} \cdot 2 - 1 \quad (III.1)$$

Figure III.1 is an example of this movement, in this case the z-axis is being forced to read the known acceleration values. The resulting data of such a movement is shown in figure III.2. Having executed the movement, the data is now registered. The next step is to discover the variables  $C_{max}$  and  $C_{min}$ . This movement must be performed slowly - in figure III.2 the movement took 30 seconds - this guarantees the accelerometer never reads more than  $+g$  or less than  $-g$ . With this, to find the variables, all that's left is to find the maximum and the minimum of the acquired data. A smoothing of the data, prior to finding the maximum and minimum, is recommended as it allows a simple script to find the maximum and minimum accurately.

After finding these values, all that's left is replacing  $C_{max}$  and  $C_{min}$  in equation III.1, and the calibration is completed.

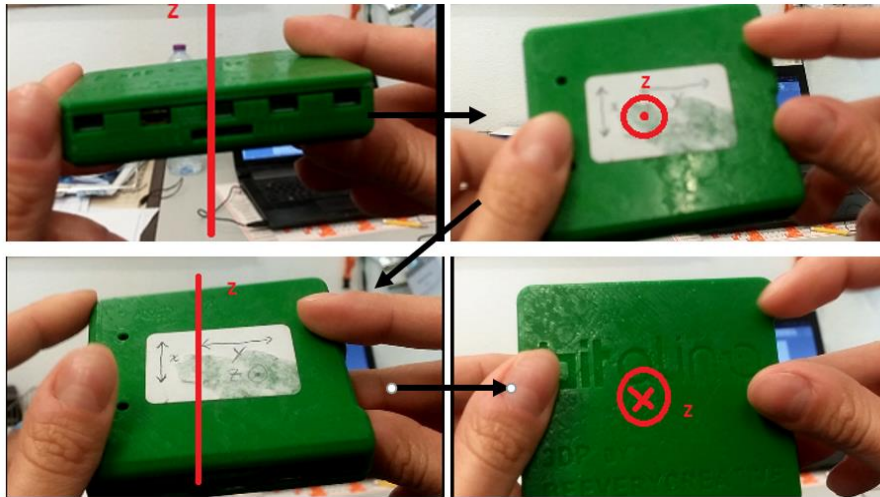


Figure III.1: Accelerometer calibration movement.

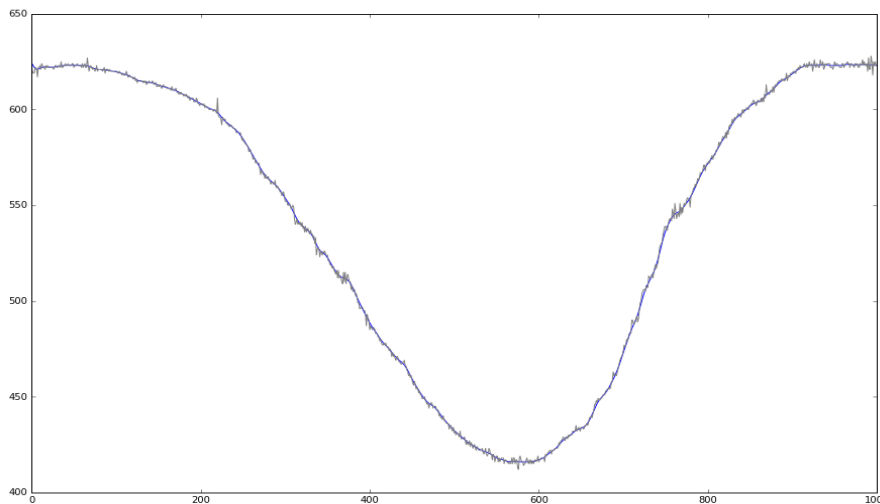


Figure III.2: Accelerometer calibration data in bits in gray. In blue the smoothed data.



## ANNEX 4 REAL PENDULUM LABORATORY GUIDE

# Movimento de um Pêndulo Real

João ALHO

8 de Setembro de 2017

Data:

Professor:

## 1 Objetivo

Este trabalho tem duas partes. Na primeira, pretende-se determinar experimentalmente a constante de tempo de amortecimento do pêndulo. Na segunda parte, pretende-se demonstrar que para um pêndulo real o período de oscilação depende do ângulo do movimento e comparar esta dependência com a expressão teórica.

## 2 Montagem Experimental

Nesta montagem será posto um pêndulo a oscilar e a sua aceleração medida por um sensor de aceleração diretamente acoplado à massa do pêndulo. Para medir a aceleração do pêndulo utiliza-se um BITalino, placa low-cost de aquisição que inclui um acelerómetro triaxial – mede aceleração em três eixos, x, y e z - e comunica com uma ligação BT a um computador.

## 3 Introdução Teórica

### 3.1 Pêndulo Ideal

A equação diferencial do movimento angular de um pêndulo com comprimento  $l$  é:

$$\frac{d^2\theta}{dt^2} + \frac{g}{l} \sin \theta = 0 \quad (1)$$

Se se considerar apenas oscilações em pequenos ângulos ( $\theta \ll 1rad$ , faz-se a chamada aproximação dos pequenos ângulos, da qual resulta:

$$\frac{d^2\theta}{dt^2} + \frac{g}{l} \theta = 0 \quad (2)$$

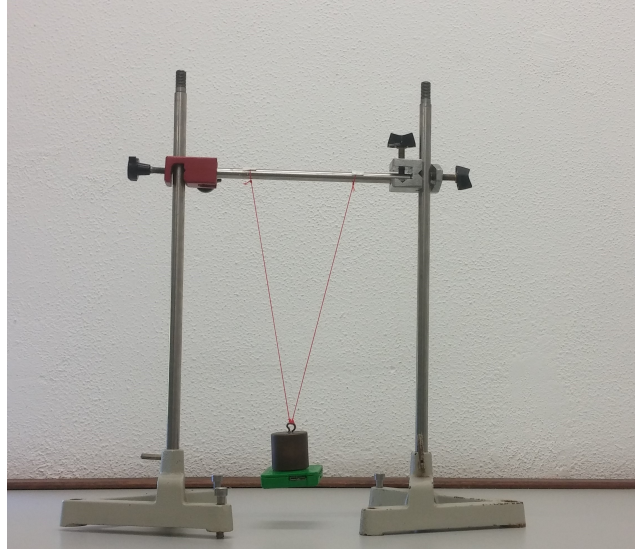


Figura 1: Montagem experimental.

Ora, a solução desta equação diferencial é a expressão 3. Aqui,  $\theta_0$  é o ângulo inicial da oscilação,  $\omega$  é velocidade angular do movimento dada por  $\sqrt{g/l}$  e  $\phi$  é uma condição inicial, que consideramos 0 no futuro.

$$\theta(t) = \theta_0 \cos(\omega t + \phi) \quad (3)$$

Visto que  $\omega = \sqrt{g/l}$ , para um pêndulo ideal de pequenas oscilações o período vem então independente do ângulo de oscilação:

$$\omega = \frac{2\pi}{T} = \sqrt{\frac{g}{l}} \implies T = 2\pi\sqrt{\frac{l}{g}} \quad (4)$$

Associado ao movimento do pêndulo, que pode ser considerado como circular, vem uma aceleração.

$$a_r = -\frac{v^2}{l} \quad (5)$$

$$a_t = l \cdot \frac{dv}{dt} \quad (6)$$

Esta aceleração terá componentes radial e tangencial dadas pelas equações 5 e 6, respetivamente. Aqui  $v$  é a velocidade instantânea do pêndulo dada pela derivada de  $\theta(t)$ , equação 7.

$$v = l \cdot \frac{d\theta}{dt} \quad (7)$$

## 3.2 Pêndulo Real

Para tratar um pêndulo ideal, é necessário ter em conta o amortecimento do pêndulo e, também, oscilações para grandes ângulos.

### 3.2.1 Amortecimento

Em primeiro lugar, muito sucintamente, o amortecimento. Vamos considerar que este amortecimento é devido a uma força de atrito viscosa <sup>1</sup>. A equação 3 considerando o amortecimento virá:

$$\theta(t) = \theta_0 \cos(\omega t + \phi) \cdot \exp^{-t/\tau} \quad (8)$$

Utilizando então a expressão da aceleração radial 5, obtêm-se a expressão da aceleração radial para um pêndulo amortecido:

$$a_r = l\theta_0^2 \cdot \exp^{-2t/\tau} \left[ \omega \sin(\omega t) - \frac{\cos(\omega t)}{\tau} \right]^2 \quad (9)$$

### 3.2.2 Período

Para um pêndulo real, não estaremos interessados em apenas pequenas oscilações. Assim, a aproximação feita na expressão 2 não tem interesse aqui. Contudo, a equação diferencial 1 não tem solução analítica. Existirá então uma solução numérica. Desta forma, pode-se deduzir que o período de um pêndulo é estimado pela série:

$$T = 2\pi \frac{l}{g} \left[ 1 + \frac{1}{16}\theta_0^2 + \frac{11}{3072}\theta_0^4 + \dots \right] \quad (10)$$

Consideremos pequenos ângulos, por exemplo  $\theta = 0.1rad$ . Substituindo na expressão acima, obtemos:

$$T = 2\pi \frac{l}{g} \left[ 1 + \frac{1}{16}0.01 + \frac{11}{3072}0.0001 + \dots \right] \quad (11)$$

Concluí-se que todos os termos que multiplicam pelo ângulo são desprezáveis, por serem muito inferiores a 1. De onde, se obtém que o período para estes ângulos pequenos é aproximadamente dado pela expressão 4.

---

<sup>1</sup>Conforme a intensidade, este amortecimento poderá ser fraco, forte, ou crítico. Neste caso, o amortecimento será considerado fraco. Por sua vez, um amortecimento fraco traduz-se, matematicamente, num termo exponencial  $e^{-t/\tau}$ , onde  $\tau$  é uma constante - chamada constante de tempo - que, neste caso, indica o tempo que demora até o ângulo de oscilação do pêndulo ser 0.37 vezes o ângulo inicial.



## 4 Procedimento Experimental

### 4.0.1 Montagem

- a. Registe a massa do pêndulo e do BITalino
- b. Fixe o BITalino na face inferior da massa
- c. Fixe os fios à haste horizontal
- d. Meça o raio do pêndulo.

### 4.0.2 Oscilação

- a. Verifique o bom funcionamento do pêndulo com a opção de gráfico em JANELA. Faça pequenas oscilações e verifique 'a olho' que a aceleração medida tem o dobro da frequência da oscilação do pêndulo.
- b. Quando estiver tudo 'ok' com o programa e a montagem, pare o programa e selecione agora a opção de gráfico em COMPLETO. Escolha uma janela de tempo adequada ( $> 2$  minutos, massas maiores precisam de um pouco mais tempo).
- c. Proceder à oscilação do sistema massa + BITalino, escolha um ângulo inicial elevado ( $> 60^\circ$ ).
- d. Quando o programa concluir a aquisição de dados, guarde os dados adquiridos.
- e. Repita os passos b) a e) para **3** massas e **3** comprimentos de pêndulo.

## 5 Tratamento de Dados

### 5.1 Determinação da constante de tempo de amortecimento

- a. Apresentar gráfico (aceleração vs tempo) da oscilação completa;
- b. Apresentar curva de máximo sobreposta ao gráfico anterior;
- c. Utilizando a equação 9 trace curvas de máximos de aceleração teóricas. **Sugestão:** A expressão 9 terá máximos e mínimos de aceleração. Os máximos são dados por:

$$a_r = l\theta_0^2\omega^2 \cdot \exp^{-2t/\tau} \quad (12)$$

- d. Ajuste os parâmetros  $\tau$  e  $\theta_0$  de modo a que as curvas teóricas se sobreponham às curvas experimentais.

- e. Compare o  $\tau$  obtido nas medições de massa diferentes. O que estaria à espera de observar?
- f. Compare o  $\tau$  obtido nas medições de comprimentos diferentes. O que estaria à espera de observar?

## 5.2 Verificação do Período

- a. Fazer um gráfico da variação do ângulo máximo de oscilação em função do tempo. **Sugestão:** a expressão 12 relaciona o máximo de aceleração com o ângulo. Considere cada oscilação como uma individual, de modo que o amortecimento é desprezável, ou seja  $\exp^{-2t/\tau} = 1$ .
- b. Determine os quocientes experimentais da expressão 10. Comente. **Sugestão:** A expressão 10 pode ser escrita como:

$$T = T_0 + T_0 \cdot \frac{1}{16} \theta_0^2 + T_0 \cdot \frac{11}{3072} \theta_0^4 \quad (13)$$

$$\frac{T - T_0}{T_0} = \frac{1}{16} \theta_0^2 + \frac{11}{3072} \theta_0^4 \quad (14)$$

onde  $T_0$  é o período de pequena oscilação. Os quocientes teóricos são  $\frac{1}{16}$  e  $\frac{11}{3072}$ .

## 6 Questionário

- **Extra!** Seria de esperar que o mínimo de aceleração radial fosse 0. Porque razão não se verifica isso?

## 7 Utilização do Programa

- a. Ao iniciar o programa escolha a opção **Pendulum**;
- b. Carregue em **BITalino** para fazer a ligação entre o BITalino e o computador. Aparecerá uma janela que lhe pede um MacAddress, verifique a etiqueta do seu BITalino e copie o código para esta janela e carregue em **Connect**;
- c. Verifique mexendo que os três eixos funcionam;
- d. Em seguida deverá configurar o gráfico. Os botões **Window** e **Complete** definem o tipo de visualização. Em modo **Window** será apresentado no gráfico os últimos segundos de aquisição, este tempo é escolhido em **Interval (s)**. Em modo **Complete** verá os dados adquiridos durante o tempo escolhido em **Interval(s)**. O indicador **Tempo (s)** mostra o tempo total de aquisição decorrido.

- e. Antes de iniciar aquisição de dados para o seu trabalho é recomendado fazer uma calibração do BITalino. Para isso pressione o botão **Calibrate**. Uma nova janela aparecerá onde poderá verificar os valores de calibração atuais.
- f. Será necessário calibrar cada um dos eixos individualmente. Pode consultar a que eixo correspondem x, y e z na etiqueta do seu BITalino.
- g. Para proceder à calibração de um eixo pressione o botão com o nome correspondente ao eixo que quer calibrar. Quando aparecer GO! Faça uma rotação completa, lentamente (cerca de 60s com algum tempo parado no início e no fim), em torno do eixo que pretende calibrar. A figura 2 exemplifica o movimento que terá de fazer.
- h. Após fazer conexão e configurar o gráfico poderá iniciar a aquisição e visualização dos dados, pressionando **Start**. Quando a aquisição é iniciada não poderá alterar a configuração do gráfico. Existe, no entanto, a opção de mostrar/esconder os eixos de aquisição e também de fazer zoom no gráfico.
- i. Poderá parar a aquisição a qualquer momento carregado em **Stop**, sendo que na opção de visualização **Complete** a aquisição para ao fim do tempo estipulado em **Intervals (s)**.
- j. 10. Para gravar os dados adquiridos prima **Save**, é necessário em primeiro lugar parar a aquisição de dados.
- k. No trabalho do pêndulo os dados são guardados em folha de Excel. Os dados fornecidos são:
  - Os pontos adquiridos durante a oscilação, unidades –  $m/s^2$ ;
  - Valor dos máximos e mínimos e respetivos tempos a que ocorrem.

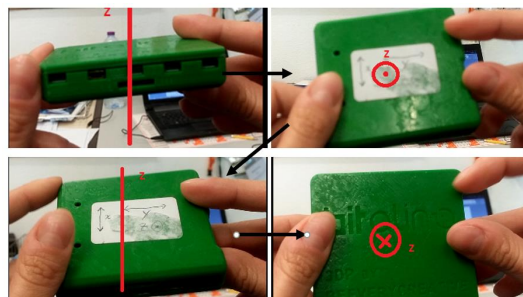


Figura 2: Exemplo do movimento de calibração para o eixo z.